



Universidade do Algarve

**Production of Nanoparticles by Polyelectrolyte Complexation from  
Novel Locust Bean Gum Cationic Derivatives**

Miguel Viegas Rodrigues

Dissertação para obtenção de grau de mestre em Ciências  
Farmacêuticas

Trabalho efetuado sob a orientação de Professora Doutora Ana Maria  
dos Santos Rosa da Costa e coorientação de Professora Doutora Ana  
Margarida Moutinho Grenha

2020



Universidade do Algarve

**Production of Nanoparticles by Polyelectrolyte Complexation  
from Novel Locust Bean Gum Cationic Derivatives**

Miguel Viegas Rodrigues

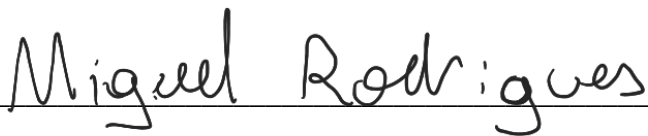
Dissertação para obtenção de grau de mestre em Ciências  
Farmacêuticas

Trabalho efetuado sob a orientação de Professora Doutora Ana Maria  
dos Santos Rosa da Costa e coorientação de Professora Doutora Ana  
Margarida Moutinho Grenha

2020

## DECLARAÇÃO DE AUTORIA DE TRABALHO

Declaro ser o autor deste trabalho, que é original e inédito. Autores e trabalhos consultados estão devidamente citados nos textos e constam da listagem de referências incluída.

  
\_\_\_\_\_

**Copyright © 2020** Miguel Viegas Rodrigues

A Universidade do Algarve tem o direito, perpétuo e sem limites geográficos, de arquivar e publicitar este trabalho através de exemplares impressos reproduzidos em papel ou de forma digital, ou por qualquer outro meio conhecido ou que venha a ser inventado, de o divulgar através de reportórios científicos e de admitir a sua cópia e distribuição com objetivos educacionais ou de investigação, não comerciais, desde que seja dado crédito ao autor e editor.

*Only through training will a person learn his own weaknesses... He who is  
aware of his weaknesses will remain master of himself in any situation.*

Gichin Funakoshi

*Education is the kindling of a flame, not the filling of a vessel.*

Socrates

## Acknowledgements

Em primeiro lugar quero agradecer à professora Ana Costa, por toda a ajuda no laboratório, na orientação desta dissertação, por ser um suporte sempre presente nesta aventura que foi a investigação, e por me ensinar, acima de tudo, perseverança.

Agradeço igualmente à professora Ana Grenha pelo convite para poder fazer parte deste projeto e pela coorientação da dissertação, e por nunca deixar de apelar à ambição dos alunos.

Estou também muito grato pela ajuda de todos os colegas que estiveram comigo no laboratório, que me ajudaram a obter resultados e me acompanharam a resmungar quando não eram o que estávamos à espera.

Quero deixar uma palavra de gratidão a todos os professores que, desde sempre, me fizeram apaixonar pelas biológicas, pelas físicas, pelas químicas e por todos os “Porquês” em geral.

Aos amigos que a universidade me deu, agradeço por sofrermos e celebrarmos.

Agradeço aos meus pais por me fazerem querer ser melhor do que ontem.

Finalmente, agradeço aos meus avôs, por me ensinarem tanta coisa, do princípio ao fim.

## Contents

Acknowledgements.....	III
Abstract.....	VI
Resumo .....	VII
Resumo Alargado .....	VIII
Abbreviations.....	XI
Figure index .....	XII
Table index .....	XIII
1 Introduction .....	1
1.1 Drug delivery .....	1
1.1.1 The importance of nanoparticles in drug delivery .....	1
1.1.2 Nanotechnology in biomedical applications.....	1
1.1.3 Nanoparticle production .....	2
1.2 Polysaccharides in drug delivery and biomedical applications .....	4
1.2.1 Alginate.....	4
1.2.2 Carrageenan .....	5
1.2.3 Cellulose .....	6
1.2.4 Chitin and Chitosan .....	7
1.2.5 Curdlan .....	8
1.2.6 Dextran .....	9
1.2.7 Fucoidan .....	10
1.2.8 Hyaluronic acid.....	11
1.2.9 Locust bean gum.....	12
1.2.10 Pullulan.....	13
1.2.11 Starch .....	13
1.3 Polysaccharides chemical modification.....	14
1.3.1 Oxidation .....	15

1.3.2	Reductive amination .....	20
1.3.3	Alkylation with ammonium quaternary salts.....	22
1.3.4	Carboxymethylation .....	23
1.3.5	Sulfation.....	25
1.3.6	Phosphorylation .....	26
2	Objectives.....	28
3	Materials and methods .....	29
3.1	Materials .....	29
3.2	Synthesis of LBG derivatives .....	29
3.2.1	Purification of LBG .....	29
3.2.2	Oxidation .....	30
3.2.3	Reductive amination .....	32
3.3	Production of ALBG/CRG nanoparticles .....	35
3.4	Characterization of ALBG/CRG nanoparticles .....	36
4	Results and discussion.....	37
4.1	Synthesis and characterization of locust bean gum derivatives.....	37
4.1.1	Oxidation of LBG .....	37
4.1.2	Reductive amination of LBG.....	41
4.2	ALBG/CRG nanoparticles .....	46
5	Conclusions and future work .....	48
6	References .....	51

## Abstract

Nanoparticles have a wide array of uses, one of which is drug delivery. Nanoparticle drug delivery systems have advantages over conventional drug delivery systems, as they are able to increase bioavailability, solubility and permeability of drugs, while also offering the possibility of targeted delivery and controlled release. The preparation of nanoparticles can follow different procedures, including polyelectrolyte complexation, based on electrostatic interaction of oppositely charged polymers, which was used in this work. There are currently a wide number of anionic polysaccharides to choose from, either from seaweed, animals or microorganisms. Still, when it comes to cationic polysaccharides, the most common choice is chitosan. For this reason, the chemical modification of polysaccharides for obtaining positively-charged derivatives is worth exploring.

The main objective of this work was to explore different strategies to chemically modify locust bean gum in order to obtain a cationic polyelectrolyte that, by complexation with carrageenan, affords nanoparticles with the potential for application in the development of drug delivery systems. To achieve this, it was attempted to oxidize locust bean gum to the corresponding aldehyde using different oxidizing reagents and then, by reductive amination, insert amino groups in the polysaccharide structural units. The different oxidation reagents were sodium periodate, TEMPO, Oxone<sup>®</sup> and ammonium persulfate. All obtained derivatives were analyzed through FTIR spectroscopy to assess the success of each reaction.

NMR analysis was also performed on amino locust bean gum obtained from periodate oxidized gum, which seemed to indicate a high degree of depolymerization during the reductive step.

Nanoparticle production was possible using amino locust bean gum obtained from periodate oxidized gum and carrageenan at mass ratios of 4/1, 1/3 and 1/4. These particles showed similar size, zeta potential and PDI as other locust bean gum based nanoparticles, albeit with a larger deviation.

**Keywords:** Locust bean gum, Nanoparticles, Polyelectrolyte complexation, Polysaccharide modification.

## Resumo

As nanopartículas têm um largo espectro de utilizações, um dos quais é a veiculação de fármacos. Sistemas de entrega de fármacos baseados em nanopartículas têm vantagens face a sistemas mais convencionais, como o aumento de biodisponibilidade, solubilidade e permeabilidade dos fármacos e ao mesmo tempo oferecem a possibilidade de orientação para alvos terapêuticos específicos e de libertação controlada. A preparação de nanopartículas é feita de diversas formas, incluindo a complexação polieletrólítica, que se baseia na interação eletrostática de polímeros de cargas opostas, a qual se utiliza neste trabalho. Atualmente há várias opções de polissacáridos aniónicos, de algas, animais ou microorganismos, enquanto uma das únicas opções de polissacárido catiónico é o quitosano. Assim sendo, existe interesse em explorar a modificação química de polissacáridos para a atribuição de cargas positivas.

O objetivo deste trabalho foi explorar diferentes estratégias de modificar a goma de alfarroba para obter um polieletrólito que se pudesse complexar com carragenina para obtenção de nanopartículas com potencial aplicação em veiculação de fármacos. Para isso, tentou-se oxidar a goma para o respetivo aldeído e, através de aminação reductiva, introduzir grupos amina nas unidades estruturais do polissacárido. A oxidação foi testada com periodato de sódio, TEMPO, Oxona<sup>®</sup> e persulfato de amónia. Os derivados foram analisados por espectroscopia FTIR para verificar o sucesso das reações.

Também foi feita caracterização por NMR da goma aminada obtida da goma oxidada com periodato, que mostrou um elevado grau de despolimerização durante o passo de redução.

A produção de nanopartículas deste derivado com carragenina foi possível e, nas razões de massa 4/1, 1/3 e 1/4 estas partículas mostravam tamanho, potencial zeta e PDI semelhantes aos de outras nanopartículas baseadas noutros derivados da goma de alfarroba.

**Palavras-chave:** Complexação de polieletrólitos, Goma de alfarroba, Modificação de polissacáridos, Nanopartículas.

## Resumo Alargado

A veiculação de fármacos é um campo de investigação relativamente novo, mas a ideia de utilizar excipientes para alterar as propriedades farmacocinéticas ou farmacodinâmicas do fármaco tem vindo a ser cada vez mais estudada. Enquanto inicialmente os excipientes numa formulação poderiam alterar, por exemplo, a velocidade de libertação de um fármaco, hoje em dia são também utilizados para direcionar os fármacos para diferentes alvos biológicos, aumentando a sua eficiência. Uma parte significativa da investigação em veiculação de fármacos atual é baseada em nanotecnologia.

A nanotecnologia refere-se originalmente a materiais entre 1 e 100 nanómetros, mas a definição foi recentemente alargada para incluir partículas de tamanho até 1 micrómetro que exibam as propriedades características das nanopartículas, como o elevado rácio de área de superfície para volume, que aumenta a sua importância da química de superfície.

As nanopartículas são utilizadas nas mais diferentes áreas, uma das quais é a veiculação de fármacos. Os sistemas de veiculação de fármacos baseados em nanopartículas possuem muitas vantagens quando comparados com outros sistemas: a sua utilização torna possível aumentar a biodisponibilidade, solubilidade e permeabilidade de fármacos e permite a sua administração através das mais diversas vias, incluindo a oral, intravenosa, tópica ou mesmo pulmonar, para veiculação de pequenas moléculas, proteínas ou genes. Para além disso, a nanotecnologia permite a modulação da libertação de fármacos, bem como a sua vetorização para alvos terapêuticos específicos.

As nanopartículas podem ser produzidas de diversas formas, sendo que uma das mais vantajosas neste contexto é a complexação polieletrólítica. Este método consiste na formação de partículas através da interação eletrostática entre um polímero positivamente carregado com um polímero negativamente carregado, e pode ser utilizado com polímeros naturais, semissintéticos ou sintéticos. Os polímeros naturais, nomeadamente polissacáridos, ou seus derivados semissintéticos, são preferíveis pela sua biocompatibilidade e sustentabilidade. Tendo isto em conta, há várias opções de polissacáridos aniónicos, de algas, animais ou microorganismos, enquanto uma das únicas opções de polissacárido catiónico é o quitosano, um derivado da quitina.

Para a produção de polímeros semissintéticos, recorre-se à modificação química de polissacáridos naturais. A modificação química de polissacáridos é um ramo importante da ciência destas moléculas que permite aumentar a sua aplicabilidade em diferentes campos, incluindo as ciências farmacêuticas ou biomédicas. A modificação química dos polímeros pode adicionar nova atividade funcional a estas moléculas pela alteração de várias propriedades físico-químicas, tais como a solubilidade em água, o peso molecular e o grau de substituição. Já estão reportadas diversas modificações de polissacáridos naturais, como a ligação a aminas quaternárias, sulfatação, fosforilação, carboximetilação, acetilação, metilação, oxidação e aminação reductiva.

Assim sendo, o objetivo deste trabalho foi estudar a modificação química da goma de alfarroba, o que valoriza um produto local, para obter um derivado catiónico que, tal como o quitosano, pudesse ser utilizado na formação de nanopartículas por complexação polieletrólítica.

A goma de alfarroba é obtida do endosperma da semente da alfarrobeira (*Ceratonia siliqua*). Tem um alto peso molecular, de 50 a 3000 kDa, e consiste numa cadeia linear de unidades 1,4- $\beta$ -D-manose com resíduos laterais de 1,6- $\alpha$ -D-galactose, sendo, portanto, um galactomanano. Este polímero já foi quimicamente modificado para obter derivados para utilização na produção de nanopartículas noutros trabalhos do grupo. O objetivo da modificação química deste polissacárido foi a introdução de grupos amina. A estratégia de modificação foi realizada em duas etapas: oxidação dos grupos hidroxilo da goma a aldeídos e aminação reductiva dos mesmos. Entre estas etapas existiu um passo de purificação por diálise e o produto final foi isolado por precipitação ou liofilização. Assim, obteve-se uma goma com aminas primárias que, em meio ácido, era positivamente carregada. O objetivo inicial foi conseguir cerca de 80% de substituição, para obter um polímero de carga semelhante ao quitosano. As reações foram testadas em diferentes condições de equivalentes de reagente, temperatura e duração e a oxidação foi feita com quatro agentes oxidantes distintos. A oxidação foi testada com periodato de sódio, TEMPO, Oxona<sup>®</sup> e persulfato de amónia.

Após cada reação, os derivados eram avaliados por espectroscopia de infravermelho com transformada de Fourier, para se estimar o grau de substituição e extensão da reação através dos picos associados ao grupo aldeído ou amina. Através desta técnica concluiu-se que a goma aminada mais bem-sucedida foi a obtida através da oxidação com quatro equivalentes de periodato de sódio.

Para este produto em específico, foi feita a caracterização por ressonância magnética nuclear, para tentar perceber a estrutura do polímero final. Esta técnica permitiu perceber que o polímero sofria despolimerização, possivelmente durante a fase de redução, o que explicou o baixo rendimento da reação.

Finalmente, foi ainda testada a produção de nanopartículas deste derivado aminado com carragenina, um polissacárido aniónico extraído de algas vermelhas. A produção de nanopartículas foi testada em diferentes rácios de massa de polímero positivo para negativo, de 4/1 a 1/4. Foi possível obter nanopartículas quando foi utilizado o derivado obtido da oxidação da goma com quatro equivalentes de periodato de sódio referido acima. As nanopartículas produzidas utilizando rácios de massa de polímero positivo para negativo de 4/1, 1/3 e 1/4 apresentaram tamanho, potencial zeta e polidispersidade semelhantes aos de outras nanopartículas constituídas por derivados carregados da goma de alfarroba, embora com uma variação superior.

Mais estudos são necessários no sentido de obter um substituto do quitosano baseado na goma de alfarroba modificada. A nível de síntese, a oxidação por diferentes reagentes deve ser mais estudada pois estes preservam mais a estrutura natural da goma de alfarroba, enquanto o periodato de sódio cliva ligações das unidades estruturais do polissacárido. A nível de condições de reação, o processo deve ser aprimorado para se obter um melhor rendimento e grau de substituição. Devem-se criar novas estratégias que ajudem na obtenção de um meio de reação mais homogéneo, recorrendo à adição de sais ou mesmo a outra técnica de purificação inicial da goma de alfarroba. Quanto à caracterização dos derivados, outras técnicas devem ser aplicadas, nomeadamente a análise elementar, que permite tirar mais conclusões quanto à estrutura final do polímero modificado. No que toca às partículas, devem ainda ser feitos testes de rendimento de produção e análise morfológica das mesmas.

## Abbreviations

**ALBG-** Amino locust bean gum

**CMC-** Carboxymethylcellulose

**CRG-** Carrageenan

**dd-** Duplet of duplets

**DMF-** Dimethylformamide

**EDC-** 1-Ethyl-3-(3-dimethylaminopropyl)carbodiimide

**FDA-** Food and Drug Administration

**FTIR-** Fourier-transform infrared

**HSQC-** Heteronuclear single quantum coherence

**J-** J-coupling

**LBG-** Locust bean gum

**m-** Multiplet

**NHS-** N-Hydroxysuccinimide

**NMR-** Nuclear magnetic resonance

**Pdi-** Polydispersion index

**siRNA:** Small interfering RNA

**TEMPO-** (2,2,6,6-Tetramethylpiperidin-1-yl)oxyl

**tt-** Triplet of triplets

## Figure index

Figure 1.1: a) <i>Laminaria digitata</i> (by David Baird) and alginate blocks containing b) mannuronate, c) guluronate and d) both.....	5
Figure 1.2: a) <i>Chondrus crispus</i> , a red algae (by Emőke Dénes) and b) kappa carrageenan structure.....	6
Figure 1.3: a) Cotton, a common cellulose source, and b) cellulose structure.....	7
Figure 1.4: Crab exoskeleton (by Charles J Sharp), one source of chitin, b) chitosan and c) chitin structures. ....	8
Figure 1.5: a) <i>Alcaligenes faecalis</i> (by CDC/ Dr. W.A. Clark - Centers for Disease Control and Prevention), gram stained, and b) curdlan structure.....	9
Figure 1.6: a) <i>Leuconostoc mesenteroides</i> (by Fred Breidt, North Carolina State University) and b) dextran structure.....	9
Figure 1.7: a) <i>Fucus vesiculosus</i> (by Emőke Dénes), one source of fucoidan; and b) common structure of fucoidan from <i>Fucales</i> order algae. R represents possible branching, acetylation and sulfation.....	10
Figure 1.8: a) Rooster comb (by Muhammad Mahdi,), a source of hyaluronic acid, and b) hyaluronic acid structure. ....	11
Figure 1.9: a) Locust bean pod and seeds (by Roger Culos) and b) locust bean gum structure. ....	12
Figure 1.10: a) <i>Aureobasidium pullulans</i> (by Tom Volk at Mushroom Observer) and b) pullulan structure.....	13
Figure 1.11: a) Corn (by Alabama Extension), a common source of starch, and b) amylose and c) amylopectin structures.....	14
Figure 1.12: Oxidation of $\beta$ -D-mannopyranose with periodate.....	15
Figure 1.13: TEMPO-mediated oxidation of $\beta$ -D-mannopyranose. ....	18
Figure 1.14: Oxidation of $\beta$ -D-mannopyranose with Oxone <sup>®</sup> .....	19
Figure 1.15: Reductive amination of $\beta$ -D-mannopyranose dialdehyde.....	20
Figure 1.16: Alkylation of $\beta$ -D-mannopyranose with glycidyltrimethylammonium chloride. ....	22
Figure 1.17: Carboxymethylation of $\beta$ -D-mannopyranose with chloroacetic acid. ....	23
Figure 1.18: Sulfation of $\beta$ -D-mannopyranose with SO <sub>3</sub> ·DMF.....	25
Figure 1.19: Phosphorylation of $\beta$ -D-mannopyranose with phosphorous acid. .	26

Figure 3.1: Nanoparticle production procedure scheme.....	36
Figure 4.1: Mechanism of periodate diol cleavage.....	37
Figure 4.2: a) FTIR spectra of LBG, LBG oxidized with 4 equivalents of periodate and ALBG. Arrows indicate the carbonyl band in oxidized LBG and that of C-N in ALBG. b) FTIR spectra of LBG, LBG oxidized with 8 equivalents of periodate and ALBG. Arrow indicates the carbonyl band in oxidized LBG. c) FTIR spectra of LBG, LBG oxidized with TEMPO and ALBG. Arrows indicate the carbonyl band in oxidized LBG and that of carboxylic acid and C-N in ALBG. d) Second derivative of the FTIR spectrum of LBG oxidized with TEMPO. The arrow points the carboxylate band. e) FTIR spectra of LBG, LBG oxidized with Oxone <sup>®</sup> and ALBG. Arrows indicate the carbonyl band in oxidized LBG and that of C-N in ALBG. f) FTIR spectra of LBG and ammonium persulfate oxidized LBG. Arrow indicates the carbonyl band in oxidized LBG. ....	38
Figure 4.3: C-6 oxidation of a $\beta$ -D-mannopyranose with a. TEMPO, b. Oxone <sup>®</sup> , c. ammonium persulfate, followed by reductive amination.....	40
Figure 4.4: Reductive amination of an aldehyde group.....	41
Figure 4.5: Oxidation by periodate and reductive amination of a $\beta$ -D-mannopyranose.....	41
Figure 4.6: a) <sup>1</sup> H and b) HSQC NMR spectra of ALBG. ....	44
Figure 4.7: Regioselective ring opening of carbohydrates in a reductive medium. ....	45
Figure 4.8: Fragments of ALBG after ring opening in reductive medium. a) and b) represent unoxidized mannose and galactose units after ring opening, c) and d) represent the fragments obtained after cleavage of oxidized mannose and e) and f) represent the fragments obtained after cleavage of oxidized galactose.....	45
Figure 4.9: Effect of ALBG/CRG mass ratio on nanoparticle size and zeta potential (mean $\pm$ SD, n = 3). ....	48

## Table index

Table 4.1: Charge ratio of ALBG/CRG nanoparticles and concentration of each polysaccharide in the mixture.....	46
Table 4.2: Physicochemical characteristics of ALBG/CRG nanoparticles (mean $\pm$ SD; n = 3). ....	47

## 1 Introduction

### 1.1 Drug delivery

#### 1.1.1 The importance of nanoparticles in drug delivery

Presently, while some still consider excipients as the pharmacologically inert elements of a formulation, it is acknowledged that these components have a role in both pharmacokinetics and pharmacodynamics (1).

Since ancient times, different medicines have been incorporated in different formulations to modify their effect on the user. Physicians would prepare medicines with different concentrations, excipients and administer them using different routes (2).

While drug delivery is a rather new field of research, the idea of using excipients to alter properties like the rate of dissolution, in order to have controlled release of drugs, was already explored in the sixteenth century by the persian physician Imad, when opium pills were made with almond oil, wax and sugar to help extend the effect of the drug, so opium addicts were able to not break their fast during Ramadan (3). As such, the ability to control the pharmacokinetics of drugs by different formulations has been remotely known for a long time. Industrially produced controlled-release drugs appeared more recently, in 1952, when Smith Klein Beecham released Dexedrine (dextroamphetamine sulfate) (4), which was a product of Spansule<sup>®</sup> technology, based on the combination of wax-coated and uncoated pellets for a particular drug release profile. This was the first of many sustained-release products based on control of dissolution or diffusion (5). Later in the century, more complicated drug delivery was applied to bigger molecules, peptides and proteins, with the most studied case being the delivery of insulin (6,7). Then, in the twenty-first century, the most explored use of drug delivery knowledge was tumor targeting (5,8). Thanks to advances in other fields of science, a significant branch of recent research in drug delivery is also based on nanotechnology (9).

#### 1.1.2 Nanotechnology in biomedical applications

Nanotechnology originally refers to the use of materials in the nanoscale range, meaning from 1 to 100 nanometers. Due to their size, these materials exhibit different physicochemical properties and biological effects comparing with the corresponding larger size forms. One such feature is the increased surface area to volume ratio, which

places more importance on the surface chemistry of these particles. As these properties are the defining attribute of nanomaterials, the Food and Drug Administration (FDA) has expanded the definition of nanomaterial to include materials out of nanoscale range, up to a micrometer, that exhibit similar properties to those of the nanoscale range (10).

Nanoparticle delivery systems are widely investigated, and have been used in various administration routes, like oral, topical, pulmonary and intravenous, for the delivery of small molecules, genes or peptides.

Oral delivery is the most common administration route but poor solubility, stability and bioavailability of many drugs can make the therapeutic effect harder to achieve. The use of nanoparticles can help protect the molecules from gastrointestinal degradation, increase bioavailability and control release and targeting different tissues (11). For intravenous administration, the use of nanosystems is a good tool for constructing targeted or triggered-released drugs, very useful in cancer treatment (12). In topical delivery, nanomaterials have been used to increase drug permeation through the skin (13). In inhalable systems, nanoparticles present the disadvantage of having inadequate aerodynamic properties to reach the lungs. Despite this, nanoparticles have been included in larger, more adequate delivery systems, to take advantage of their large contact surface with cells and ability to be modified and used in targeted delivery (14).

Nanosystems are useful in gene therapy, both as DNA or RNA carriers, as they are an alternative to viral vectors, producing a decreased immune response and having more design flexibility, as they can be functionalized and targeted to different sites (15). In addition, while viral vectors have a small volume and, therefore, limited loading capacity, nanomaterials can be used to carry larger nucleic acid molecules (16). In peptide and protein delivery, nanotechnology similarly plays an important role as it is a tool to circumvent the problems of protein administration, like its susceptibility to enzymatic degradation and limited cellular internalization, while also enabling different protein administration routes, like oral, nasal, pulmonary and transdermal, to be effectively used (17).

### 1.1.3 Nanoparticle production

Nanoparticles can be classified according to their various dimensions, shapes and materials. Their morphology can be spherical, cylindrical, tubular, conical, spiral, flat,

amongst other shapes, with regular or irregular surfaces and a crystalline or amorphous structure. According to the materials they are produced from, nanoparticles can be either inorganic or organic. Inorganic nanoparticles are often metal- or metal oxide-based. Organic nanoparticles are usually polymer based or lipid based, and present good biodegradability and low toxicity, making these ideal candidates for drug delivery. A third group of nanoparticles can be considered, the carbon-based nanoparticles, made entirely of carbon atoms, like fullerene, graphene and carbon nano tubes or fibers (18–20). Production methods of nanoparticles are dependent on the used materials and also determinant for the physicochemical properties of the particles. Top down (destructive) and bottom up (constructive) methods can be considered, meaning that nanoparticles can be produced by either reducing a bulk material to the nanometric scale or by building nanoparticles by clustering of matter below the nanometric scale (19).

When it comes to polymers, two common bottom up methods for nanoparticle production are ionic gelation and polyelectrolyte complexation, both based on electrostatic interactions (21,22). Ionic gelation relies on the ability of polyelectrolytes to crosslink in the presence of ions, as it happens with alginate (23) and chitosan (24). Meanwhile, polyelectrolyte complexation refers to the interaction between two different, oppositely charged, polymers, immediately creating particles. These two methods can be used together in order to obtain particles with better physicochemical properties through the addition of crosslinking agents (25–27).

Polyelectrolyte complexation is a popular nanoparticle production method, as it is performed in a very mild environment, usually an aqueous solution under mild stirring. This production method can be done using synthetic, natural polymers or semi-synthetic polymers (which refers to chemically modified polysaccharides) (28). Therefore, it is widely used with charged natural or functionalized polysaccharides in different formulations (29–32). While anionic polysaccharides are common, when it comes to cationic polysaccharides, usually the only option is chitosan (33), which means that the functionalization of other polysaccharides to obtain cationic derivatives is a valuable research goal.

## 1.2 Polysaccharides in drug delivery and biomedical applications

Natural materials have been accepted in a wide range of applications, including the biomedical field, being used as a replacement for synthetic materials, as they generally are biodegradable, sustainable, abundant and cost-effective (34,35).

Polysaccharides are a natural material composed of monosaccharides, the simplest carbohydrate units, joined by O-glycosidic linkages, and the different types of monosaccharides and linking between them allows for different physicochemical properties in this group of macromolecules (36). These natural polymers can be extracted from animals, plants, algae, fungi and bacteria, using different procedures resorting to hot water, alkali solution, enzymes or different solvents (37).

Currently, polysaccharides are extremely useful in drug, gene and protein delivery, cell encapsulation, wound healing and tissue engineering (38).

### 1.2.1 Alginate

Alginate is an anionic polysaccharide obtained from brown algae, *Phaeophyceae* class, including various seaweeds from the *Laminaria* genus (Figure 1.1), *Asophyllum nodosum* and *Macrocystis pyrtifera*. The polymer is isolated by treatment with an alkali solution, and filtration followed by precipitation with a salt, usually sodium or calcium chloride, obtaining the alginate salt. Alternatively, alginate bacterial biosynthesis is also a source of the polymer (39,40).

Alginate is a group of linear copolymers containing blocks of (1,4)-linked  $\beta$ -D-mannuronate and  $\alpha$ -L-guluronate residues. Blocks may be composed of repeats of one of the residues, or alternating mannuronate and guluronate residues (Figure 1.1). Alginate constitution differs based on its origin.

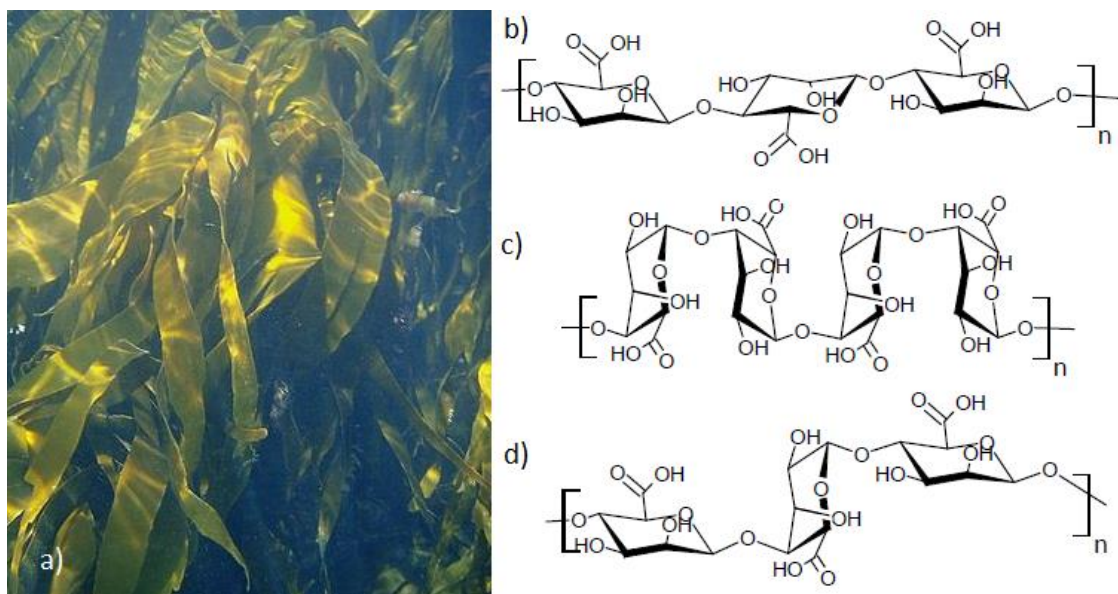


Figure 1.1: a) *Laminaria digitata* (by David Baird) and alginate blocks containing b) mannuronate, c) guluronate and d) both.

The polymer is well known for its gelation capacity in the presence of divalent cations like  $\text{Ca}^{2+}$ , possibly caused by crosslinking of the guluronate residues (40). Alginate also has mucoadhesive properties, and is considered non-toxic, biodegradable, biocompatible and non-immunogenic. These characteristics, along with its availability and low cost, make it a widely used polymer in different biomedical applications like micro and nano drug delivery systems (41), wound healing and cartilage or bone regeneration (42) and even as a bioink for 3 dimensional tissue bioprinting (43). Its structure also lends itself to chemical modification and tailoring through different reactions through the hydroxyl or carboxyl groups (44).

### 1.2.2 Carrageenan

Carrageenan refers to the gel-forming polysaccharides obtained from the extraction of some red seaweeds of the class *Rhodophyceae*. The polysaccharide is a sulfated polygalactan with 15 to 40% sulfate ester content and high molecular weight (average above 100 kDa). It is formed by alternate units of D-galactose and 3,6-anhydrogalactose joined by  $\alpha$ -1,3 and  $\beta$ -1,4-glycosidic linkages (Figure 1.2). Some structural differences, such as the number and position of sulfate ester groups and content of anhydro-galactose, affect the polymer's physical properties, such as solubility. For that reason, carrageenan can be classified in different types, from which one of the most

commonly used is  $\kappa$ -carrageenan, with a sulfate ester content of 25 to 30 wt% and an anhydro-galactose content of 28 to 35 wt% (45).



Figure 1.2: a) *Chondrus crispus*, a red algae (by Emőke Dénes) and b) kappa carrageenan structure.

Like most sulfated polysaccharides, carrageenan exhibits biological activities such as anticoagulant activity (46). Unfortunately, the polymer also seems to have inflammatory capacity (47).

Applications to the pharmaceutical field are vast, considering its negative charge and gelling properties. It can be used as a matrix in extended-release tablets (48), as a gelling agent or viscosity enhancer (49) and as a carrier or stabilizer in micro (50) or nanoparticles systems (25,51). It has been employed in the delivery of small drug molecules, macromolecules and cells (52).

### 1.2.3 Cellulose

Cellulose is by far the most common polysaccharide, being the most important skeletal component of plants. It consists of repeating  $\beta$ -D-glucopyranose molecules linked through  $\beta$ -1,4 bonds (Figure 1.3). Due to its physicochemical structure, it is unchanged when passing through the digestive tract. It can be isolated from plants, some fungus, algae and bacteria (53,54).

Isolated cellulose chains are highly hydrophilic, but these chains usually form microfibrils with dimensions from 5 to 50 nm due to hydrogen bonding. Cellulose can present different alomorphs that are classified as cellulose I $\alpha$ , I $\beta$ , II, III $\text{I}$ , III $\text{II}$ , IV $\text{I}$ , IV $\text{II}$ , with I being the native forms and the more crystalline ones (54–56).

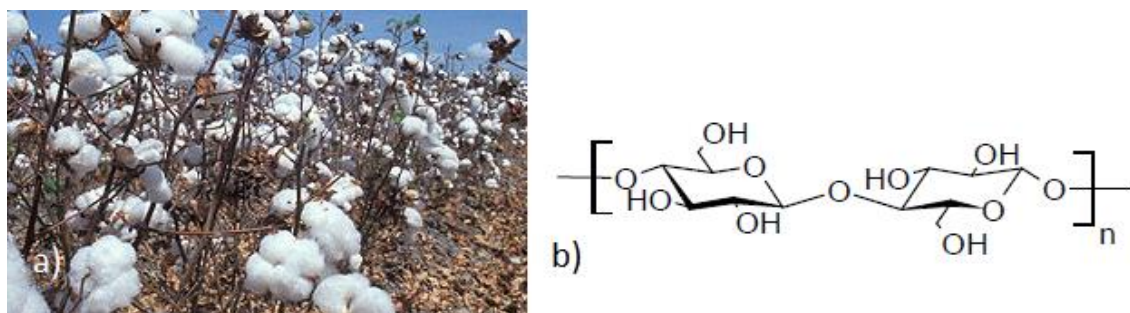


Figure 1.3: a) Cotton, a common cellulose source, and b) cellulose structure.

Cellulose nanocrystals and nanofibrils are two common cellulose products used in biomedical applications. Cellulose nanocrystals are produced by acid hydrolysis, with different acids yielding slightly different products (57–59). Meanwhile, cellulose nanofibrils are created by mechanical treatment of cellulose (60,61). Considering their biocompatibility, biodegradability, and modifiable surface, these structures have been utilized in drug delivery (62,63) and even as tissue engineering scaffolding (64).

#### 1.2.4 Chitin and Chitosan

Chitin is a natural polysaccharide, synthesized by an abundance of species, being the second most abundant natural polymer after cellulose. Its major commercial source are crab and shrimp shells, but chitin is also present in the exoskeleton of most other arthropods and in cell walls of fungi and yeasts. Chitin extraction is mainly done by acid treatment, to dissolve carbonate, followed by an alkaline solution to dissolve protein remnants (53,65,66).

Chitin is a long chain polymer of  $\beta$ -1,4-*N*-acetyl-D-glucosamines (Figure 1.4 a) and its lack of solubility is a major problem in native chitin applications. Therefore, most applications rely on chitosan, a derivative of chitin usually obtained after its partial deacetylation under alkaline conditions. Chitosan is composed of both  $\beta$ -1,4-*N*-acetyl-D-glucosamines and  $\beta$ -1,4-D-glucosamines (Figure 1.4 b), in variable proportions according to the degree of acetylation. The most used chitosan is around 20% acetylated and is soluble in acidic aqueous media due to the presence of amine groups (53,66).

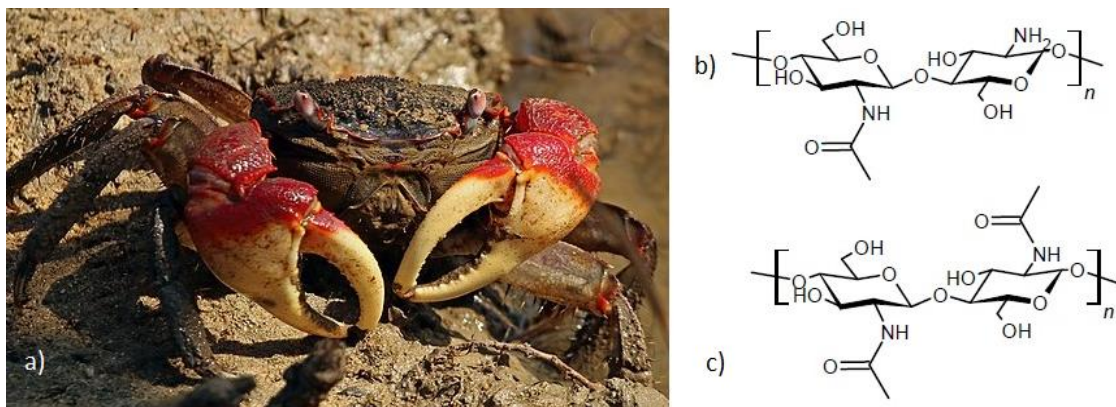


Figure 1.4: Crab exoskeleton (by Charles J Sharp), one source of chitin, b) chitosan and c) chitin structures.

Chitosan is a non-toxic and biocompatible polymer with antibacterial, antifungal, antioxidant, anti-inflammatory and antitumoral properties. It is renowned for its mucoadhesive properties and gelling capabilities, and it is vastly used in biomedical fields (65,67–73). Chitosan is a very useful polysaccharide in nanosystems assembly, as it is the only naturally occurring cationic polysaccharide, thus being an important constituent of various carriers produced by polyelectrolyte complexation (22,29,74,75). Besides, it is also used in other delivery systems, such as microspheres, as reported by Cunha *et al.* (76), tablets, micelles and hydrogels (70).

### 1.2.5 Curdlan

Curdlan is a neutral, linear chain, of as many as 12000 β-1,3-D-glucoses (Figure 1.5), that may have some intra- or inter-chain 1,6 linkages (77,78). It is produced by different microbes, including *Alcaligenes faecalis* var. *myxogenes* 0C3 strain. Curdlan is insoluble in water and mildly soluble in alkaline media (79). This polysaccharide is well-known for its thermoreversible unique gelling capabilities (80).

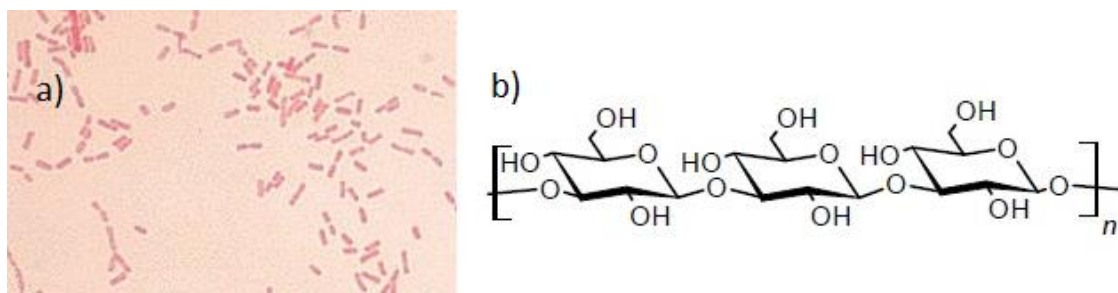


Figure 1.5: a) *Alcaligenes faecalis* (by CDC/ Dr. W.A. Clark - Centers for Disease Control and Prevention), gram stained, and b) curdlan structure.

The polysaccharide has recently been shown to have some immunostimulatory potential (81,82). Still, curdlan applications in the pharmaceutical field are mostly dependent on further functionalization and chemical tinkering to improve water solubility and bioactivity (83–86).

### 1.2.6 Dextran

Dextran refers to the group of neutral polysaccharides containing a backbone of predominantly 1,6-linked  $\alpha$ -D-glucose units (87) (Figure 1.6). Commercial dextran is usually produced by growing lactic acid bacteria, mainly *Leuconostoc mesenteroides*, in sucrose rich media (88,89), which it converts into fructose and dextran (90). The polysaccharide is then isolated and purified by precipitation in ethanol (91).

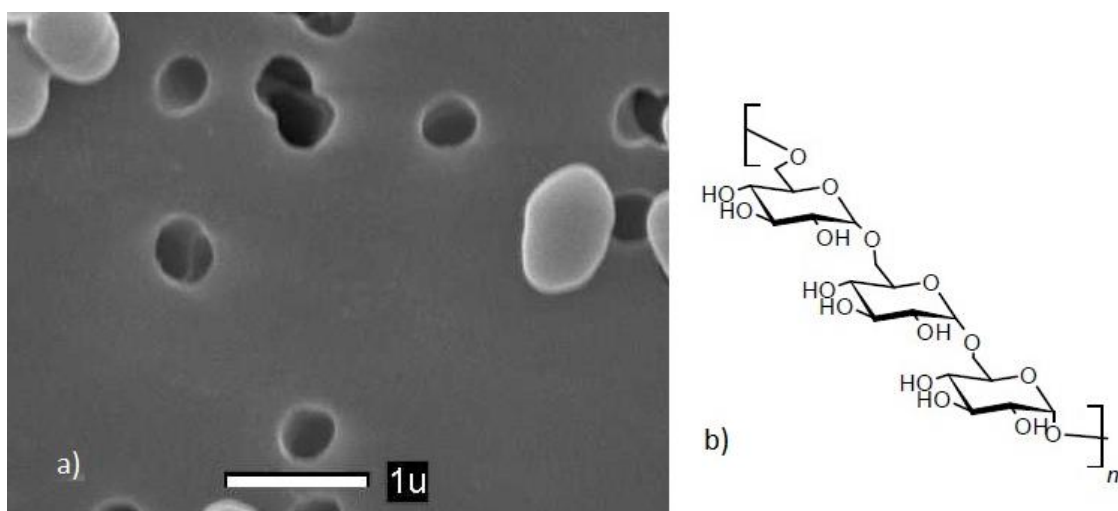


Figure 1.6: a) *Leuconostoc mesenteroides* (by Fred Breidt, North Carolina State University) and b) dextran structure.

Dextran is water-soluble and stable under both mildly acidic and basic conditions (92). It is useful in many biomedical applications because it is slowly degraded by human enzymes and microbial enzymes in the gastrointestinal tract (93).

This polymer has been traditionally used as a plasma volume expander (94), but recently it has found its uses in drug delivery, in part thanks to the development of nanosciences (95). Dextran and its sulphated counterpart have been applied to different drug delivery systems, like hydrogels, micro and nanoparticles, micelles, and vesicular nanoscaffolds (96–100).

### 1.2.7 Fucoidan

Fucoidans are a class of sulfated polysaccharides that are constituents of brown seaweed. Fucoidan is composed of  $\alpha$ -1,3 and  $\alpha$ -1,4 linked L-fucose. Some species may have a variable degree of branching, O-acetylation and even contain other monosaccharides (Figure 1.7) (101–104).

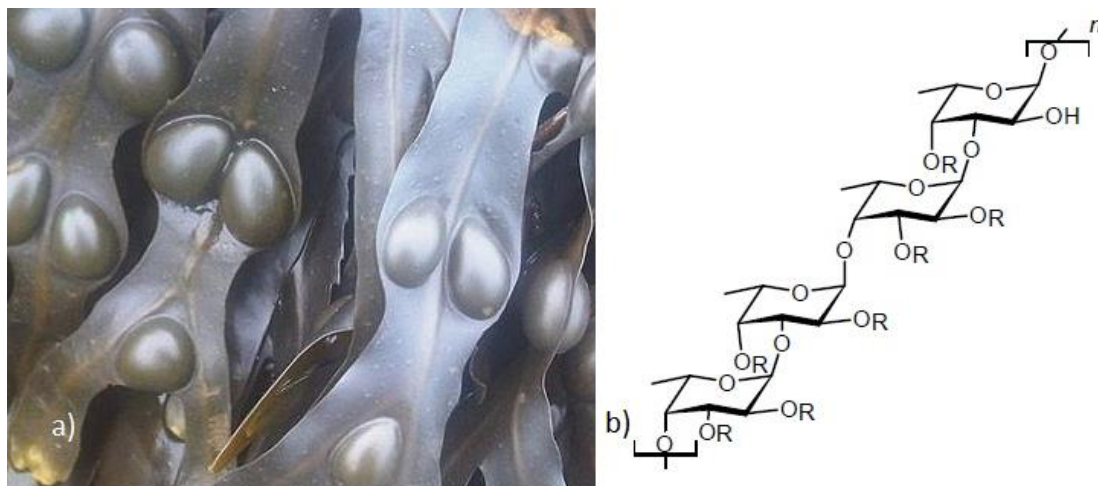


Figure 1.7: a) *Fucus vesiculosus* (by Emőke Dénes), one source of fucoidan; and b) common structure of fucoidan from *Fucales* order algae. R represents possible branching, acetylation and sulfation.

Like most sulphated polysaccharides, fucoidan presents anticoagulant properties (105). Some fucoidans have been shown to have antiviral (106,107), antioxidant (108), immunomodulatory (109) and anti-inflammatory (110) properties. It has also been researched about its hepatoprotective (111), gastroprotective (112), renal protective (113) and hypolipidemic effects (114).

Fucoidan has been used in drug delivery and chemically modified for biomedical applications (115). It was employed in a variety of micro and nanoparticle systems for anticancer therapy (116), as well as antibacterial therapy for tuberculosis (32,117), recently explored by our research group.

### 1.2.8 Hyaluronic acid

Hyaluronic acid is a linear polysaccharide composed of 2000 to 2500 disaccharide units of glucuronic acid and *N*-acetylglucosamine joined alternately by  $\beta$ -1-3 and  $\beta$ -1-4 glycosidic bonds (Figure 1.8) (118,119). Hyaluronic acid is a naturally occurring polymer in various animal tissues, including umbilical cords, synovial fluid, cartilage, skin and rooster combs, the latter being the most traditionally used and accepted source for industrial purposes. However, presently, alternative hyaluronic acid sources like *Streptococcus* capsules have also been accepted (119,120).

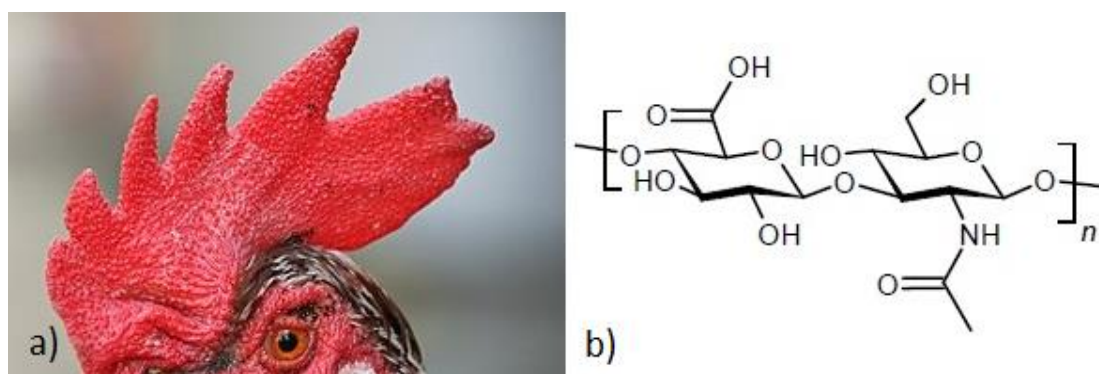


Figure 1.8: a) Rooster comb (by Muhammad Mahdi), a source of hyaluronic acid, and b) hyaluronic acid structure.

As hyaluronic acid is naturally present in synovial tissue, its use in orthopaedics is one of its classic applications. Hyaluronic acid is important in tissue hydration and in the increase of tissue resistance to mechanical stress. The polymer is shown to promote the synthesis of cartilage matrix while preventing its degradation and inflammation (121–123).

Along with being suitable for chemical modification, hyaluronic acid has good biocompatibility, biodegradability, high viscoelasticity, and can bind to specific receptor on the cell surface as a signalling molecule for inflammatory regulation (124,125). Taking this into account, this polymer has recently been used in cancer targeting (126,127) and

protein and gene delivery (128,129). Its versatility is apparent in the different systems it can incorporate, like hydrogels, microparticles and nanoparticles (130).

### 1.2.9 Locust bean gum

Locust bean gum is obtained from the endosperm of the seed of the locust tree *Ceratonia siliqua* (Fam. *Leguminosae*), a large evergreen tree. Its fruits are long brown pods from where the seeds are collected, dehusked and have the germ removed, to obtain the gum, which can be clarified. The gum consists mainly of high molecular weight (approximately 50-3000 kDa) polysaccharides with a linear chain of 1,4-linked  $\beta$ -D-mannose units with 1,6-linked  $\alpha$ -D-galactose residues as side chains (Figure 1.9). The gum is a white to yellowish white, nearly odorless powder, insoluble in most organic solvents including ethanol and partially soluble in water at room temperature and soluble in hot (85°C) water (131).

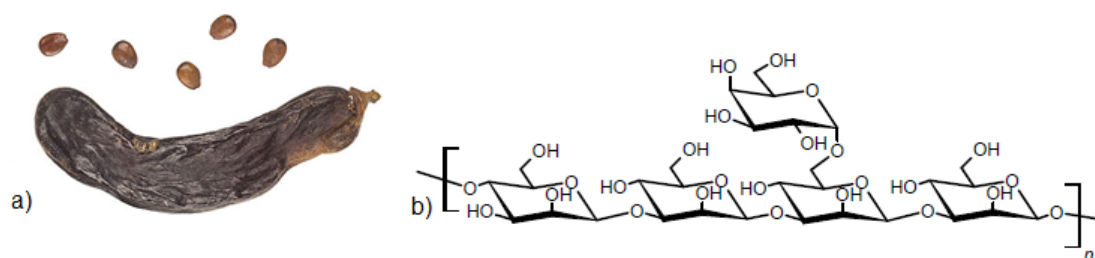


Figure 1.9: a) Locust bean pod and seeds (by Roger Culos) and b) locust bean gum structure.

The gum is a thickener and stabilizer that is used to give viscosity when added to different products, improving properties like texture, through water phase management. Therefore, it is widely used in food, as well as in the cosmetics industries (132). This polysaccharide is also used in biopharmaceutical applications, exhibiting useful properties like a high gelling capacity (133), as a controlled release excipient (134) in various delivery systems, or as a tablet disintegrant, usually associated with other polysaccharides, namely carrageenan (135). Locust bean gum also showed promising results as a substrate for some charged derivatives synthesis (30,74).

### 1.2.10 Pullulan

Pullulan is a polysaccharide secreted by the fungus *Aureobasidium pullulans*. It is composed of a linear structure of  $\alpha$ -1,6 linked maltotriose units (three glucose units linked by  $\alpha$ -1,4 bonds) (Figure 1.10) (136,137). It is highly soluble in water and insoluble in organic solvents, except for dimethylsulfoxide and formamide. It is considered non-toxic, non-mutagenic and non-carcinogenic. It presents considerable mechanical strength, adhesive properties, film formation properties and is biodegradable (138,139).

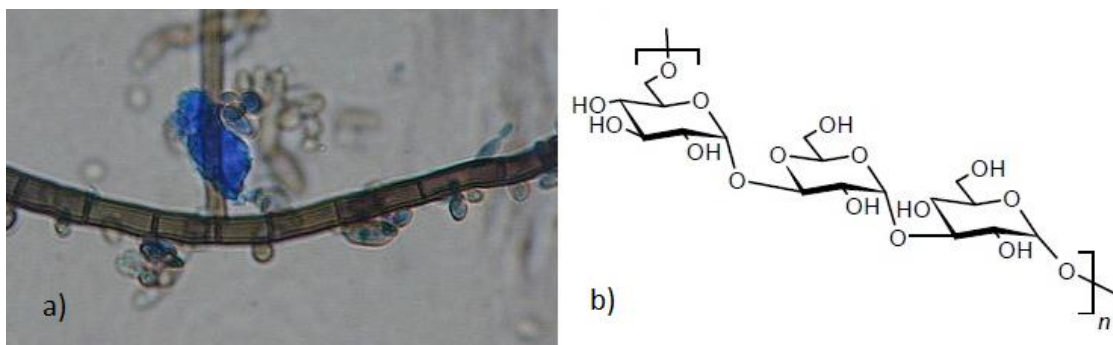


Figure 1.10: a) *Aureobasidium pullulans* (by Tom Volk at Mushroom Observer) and b) pullulan structure.

This polymer and its derivatives have been used in different biomedical applications. It has been recently used for drug and gene delivery in different forms, like nanoparticles and microspheres, being useful for targeting tumor cells (140–144). Nanoparticles produced by polyelectrolyte complexation of charged pullulan derivatives have also been reported as a carrier for the delivery of proteins by our research group (31,145).

### 1.2.11 Starch

Starch is the major dietary source of carbohydrates and the most common storage polysaccharide in plants. It exists as granules in the chloroplast of leaves and in the amyloplast of seeds, pulses and tubers. This polysaccharide is a co-polymer, and consists of 15 to 20% amylose, a linear chain of  $\alpha$ -1,4 linked D-glucose, and amylopectin, a larger branched polymer made of  $\alpha$ -1,4 and  $\alpha$ -1,6 linked D-glucose (Figure 1.11) (146).

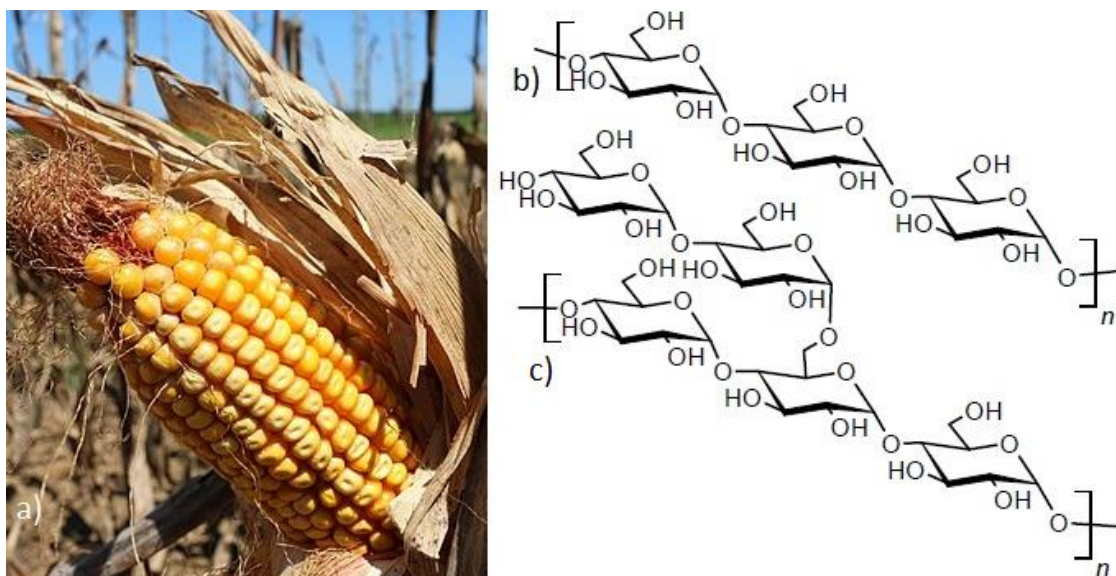


Figure 1.11: a) Corn (by Alabama Extension), a common source of starch, and b) amylose and c) amylopectin structures.

Due to its nontoxic properties, as well as its low cost and availability, starch is one of the most commonly used polymers in pharmaceutical applications as an excipient, diluent, disintegrant, binder or lubricant (147). Despite this, new functions have recently been granted to this common polysaccharide and its various derivatives (148). As such, drug delivery systems based on starch have recently been studied, including micro and nanoparticles (149–152).

### 1.3 Polysaccharides chemical modification

Polysaccharides modification is an important branch of polysaccharide science, and is done resorting to chemical, physical and biological modification methods, from which the chemical modifications are the most widely used (153). Chemical modification can add new functional activities to these molecules, by modification of physicochemical properties like water solubility, molecular weight, degree of substitution and conformation of the main polysaccharide chain (154). Functionalization of polysaccharides is, therefore, able to extend the application of bioactive materials to different areas, including biomedical areas, and design cost-effective alternatives based around non-bioactive polysaccharides (155).

### 1.3.1 Oxidation

Oxidation is a common approach in polysaccharide functionalization, in particular for controlled drug delivery purposes, in order to modulate polymer degradation to better suit its purpose (115). Different oxidizing agents may be employed, such as periodate, TEMPO and Oxone<sup>®</sup>.

#### 1.3.1.1 Periodate

Periodate oxidation can be applied to molecules with two adjacent hydroxyl groups (vicinal diols) which are or can adopt a *cis*-oriented conformation or, less effectively, equatorial trans-oriented conformation. This reaction is referred to as an oxidative cleavage, as it cleaves the bond between the two diol carbons, originating two equivalents of aldehyde (Figure 1.12). This oxidation method discerns from others, as it does not produce carboxylic acids. This reaction is valuable in polysaccharide chemistry, as polysaccharides contain several *cis*-diols and equatorial *trans*-diols, and its mild conditions in aqueous media makes this reaction easy to apply (156).

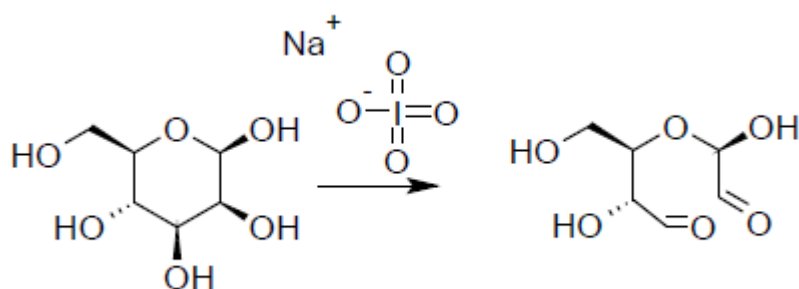


Figure 1.12: Oxidation of  $\beta$ -D-mannopyranose with periodate.

Obtaining an aldehyde can be an important intermediate step in the synthesis of other compounds. Dextran was oxidized with sodium periodate at room temperature in the dark, obtaining dextran dialdehyde, that was then conjugated with cholic acid hydrazide. Cholic acid hydrazide was produced by esterification of cholic acid with ethanol to obtain cholic acid acetate, which reacted with hydrazide monohydrate. Cholic acid hydrazide in DMF was added to an aqueous solution of oxidized dextran, stirred at 30°C for 24h and filtered. The polymer was precipitated in methanol, dissolved in DMSO and dialysed. The product was used to form nanoparticles in aqueous solution (157).

Cellulose can be oxidized with periodate to obtain an open ringed structure product. This allows for linking of other functional groups through the aldehyde, like amino groups. Zhang *et al.* used this strategy to graft silver nanoparticles with amino groups to cotton, creating a fabric with excellent antibacterial properties. The fabric was prepared by immersing cotton in a sodium periodate solution (2 g/L) at 40°C for 30 min, washing it and immersing it in a solution of silver nanoparticles for 30 min at room temperature, washing again and drying (158). Likewise, carboxymethyl cellulose (CMC) has also been oxidized with periodate to obtain dialdehyde CMC that was then crosslinked with chitosan to form a full-polysaccharide membrane in which silver ions were reduced with sodium borohydride to obtain silver nanocomposites with antibacterial properties (159).

Alginate is another polysaccharide that has been modified with periodate. After 24 h of reaction at room temperature in the dark, oxidized alginate was dialyzed. This alginate derivative was used to design prodrug nanogels for cancer diagnostic and treatment. This was followed by grafting the oxidized aldehyde with folate-terminated poly(ethyleneglycol) and rhodamine B-terminated poly(ethyleneglycol) using carbodiimide chemistry. To obtain the nanogel, the modified polymer was crosslinked using cystamine. Finally, doxorubicin hydrochloride loading was performed via acid-labile Schiff base bond. This created a carrier for doxorubicin that could be taken up by tumor cells through Folate-Receptor-mediated endocytosis and release was triggered in contact with the reductant and acid environment in the tumor, releasing the drug and emitting a strong fluorescence due to rhodamine B (160). The modification with periodate is essential in this system, as it enables control over chain length and creates more derivable groups.

Carboxymethyl pullulan, a pullulan derivative, was oxidized with sodium periodate for 24 h at room temperature, protected from light. The remaining periodate was inactivated by reaction with ethyleneglycol and the product dialysed. The modified polysaccharide was then used for production of nanoparticles, through reaction with difunctional JEFFAMINE® polyetheramines for application in the biomedical area (161).

Hyaluronic acid can be oxidized with periodate, for 2 h at room temperature in the dark before quenching the reaction with ethyleneglycol, to obtain aldehyde hyaluronic acid. This derivative can be used alongside N,O-carboxymethyl chitosan to create a hydrogel. The gel results from crosslinking of amino groups of N,O-carboxymethyl

chitosan with aldehyde groups of aldehyde hyaluronic acid. The hydrogel was successful in preventing post-operative peritoneal adhesions, according to a rat model (162).

Dialdehyde starch has also been synthesized using sodium periodate. This modified starch was then cross-linked with phosphoryl chloride in water-in-oil micro-emulsion to obtain dialdehyde starch nanoparticles to be used as a carrier for fluoruracil.

As seen by the approaches described, periodate oxidation is a very useful tool, especially when followed by crosslinking or grafting reactions, as the aldehyde groups make the substrate more reactive. The formation of aldehyde groups in polysaccharides is also an indispensable step in the preparation of the polymers for insertion of amine groups by reductive amination, as exemplified in 1.3.2.

#### 1.3.1.2 TEMPO

Oxidation with 2,2,6,6-tetramethyl-1-piperidinyloxy free radical (TEMPO) is also a very common chemical reaction in polysaccharide chemistry. In aqueous media, TEMPO is oxidized by the stoichiometric oxidant (usually sodium hypochlorite) to generate a nitrosonium cation, which is the actual oxidant of the alcohol. During the oxidation of the alcohol group of the carbohydrate, the cation is reduced to a hydroxylamine. The hydroxylamine is then reoxidized back to a nitrosonium ion completing the catalytic cycle. In a first cycle, the alcohol is converted to aldehyde and, in a subsequent one, completion of the oxidation to carboxylic acid is achieved. Hypochlorite is usually employed as primary oxidant, with bromide as a co-catalyst, as shown in Figure 1.13 (163).

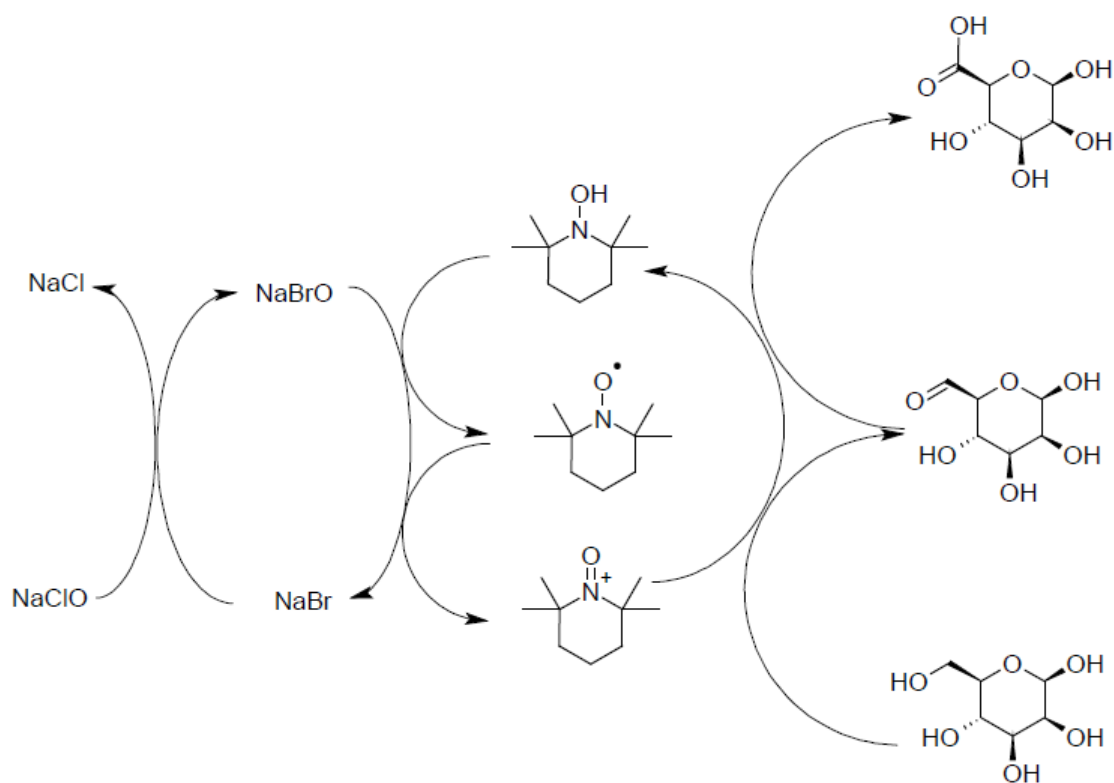


Figure 1.13: TEMPO-mediated oxidation of  $\beta$ -D-mannopyranose.

Cellulose has been successfully modified to have carboxylate groups by using TEMPO-mediated oxidation (164). The reaction was performed at room temperature, at pH=10, using sodium bromide and sodium hypochlorite. Reaction times of 1, 2, 4 and 8 h yielded progressively higher carboxylate ratios, identified by electric conductivity titration. The obtained product after 1 h reaction, in the form of sodium carboxylate cellulose, was immersed in a silver nitrate solution to obtain silver carboxylate cellulose. *In situ* thermal reduction of the silver cations enabled the formation of silver nanoparticles along the cellulose structure. These silver-associated cellulose pellicles displayed high antibacterial activity against *E. coli* and *S. aureus* and high biocompatibility, making this product a viable tool for wound dressing.

TEMPO-mediated oxidation of cellulose was also employed for the production of a drug delivery system consisting of cellulose carboxylate and aminated nanodextran combined with modified graphene oxide through electrostatic interaction forming layered nanocomposites for carrying curcumin, to be used in anticancer therapy. Drug release was engineered to be triggered by acidic environment or near infrared stimuli (165).

Locust bean gum was successfully oxidized with TEMPO, sodium hypochloride and sodium bromide, at pH=9.3, yielding an anionic polysaccharide to be used in nanoparticle production for drug delivery purposes, by polyelectrolyte complexation with a cationic locust bean gum derivative (74).

Starch was also modified by TEMPO, sodium hypochloride and sodium bromide, with pH=9.5. Ultrasonication of this starch derivative promoted the formation of carboxylate starch nanoparticles. These nanoparticles are able to interact with proteins, therefore having potential applications as nano drug carriers (166)

Carboxylic curdlan was similarly oxidized with 4-acetamido-TEMPO. The reaction proceeds similarly, but using a 4-acetamido-TEMPO/NaClO/NaClO<sub>2</sub> system under acidic conditions (pH=4,8) (167). This compound was later modified by the linkage of deoxycholic acid, creating an amphiphilic curdlan derivative. This derivative self-aggregated, forming nanoparticles that could be used for carrying hydrophobic drugs, like doxorubicin (83).

### 1.3.1.3 Oxone<sup>®</sup>

Oxone<sup>®</sup> is a trade name referring to the triple salt 2KHSO<sub>5</sub>·KHSO<sub>4</sub>·K<sub>2</sub>SO<sub>4</sub>, a high stability form of potassium peroxymonosulfate, the potassium salt of peroxymonosulfuric acid, also known as Caro's acid. This compound serves as a stoichiometric oxidizing agent under a variety of conditions, including aqueous solutions (Figure 1.14) (168).

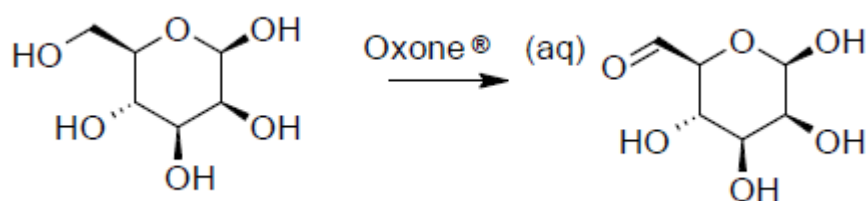


Figure 1.14: Oxidation of β-D-mannopyranose with Oxone<sup>®</sup>.

Oxone<sup>®</sup> was used to oxidize cellulose, producing cellulose nanofibers. Cellulose was dispersed in water by ultrasonication and 2.4 equivalents of Oxone<sup>®</sup> were added. After 24 h at 80°C, the oxidized cellulose was filtered. This modified polysaccharide

contained over 80% carboxylate. After mechanical treatment of the cellulose derivative, cellulose nanofibers were obtained (169).

### 1.3.2 Reductive amination

Reductive amination is an important tool for the creation of new carbon-nitrogen bonds. It is based on the condensation of an aldehyde or ketone with an amine, followed by the reduction of the resulting imine, as represented in Figure 1.15 (170). Various polysaccharides may be turned into amines by use of this reaction.

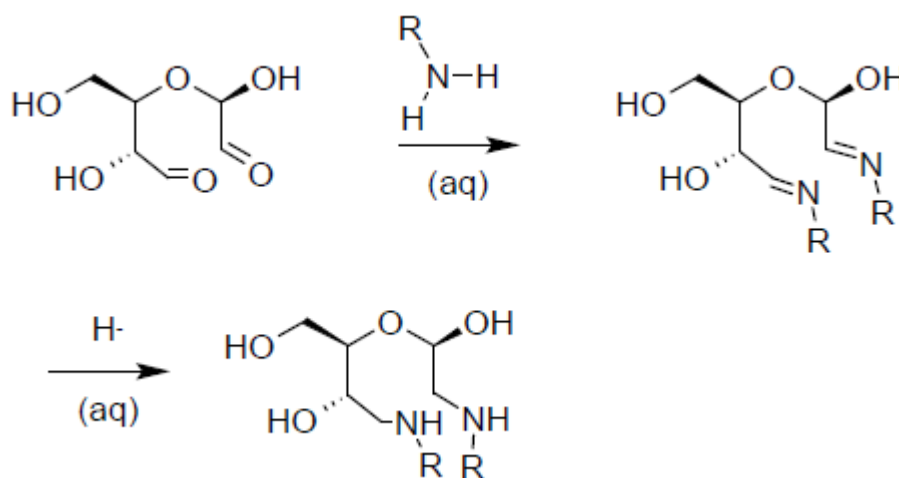


Figure 1.15: Reductive amination of  $\beta$ -D-mannopyranose dialdehyde.

Reductive amination was used to create nanowhiskey-based drug delivery systems. Cellulose nanowhiskeys were prepared by sulfuric acid hydrolysis of bleached softwood pulp, then oxidized with sodium periodate to introduce aldehyde groups. Finally, a suspension of cellulose dialdehyde was mixed with acetate buffer (pH=9) and 10 equivalents of  $\gamma$ -aminobutyric acid were added. The mixture was stirred for 24 h at 45 °C and the resulting imine was reduced *in situ* with 2.5 equivalents of sodium cyanoborohydride. After dialysis and lyophilization, the dry product was obtained with a 80-90% yield. The nanowhiskeys were further modified by esterification of the aminobutyric acid residue with a syringyl alcohol linker. This design presents a carrier molecule to be adapted for delivery of enzymes, proteins and drugs, by selecting different linker molecules (171).

Alginate was modified with periodate oxidation followed by reductive amination to link it to 4-pentyn-1-amine. After oxidation, the polysaccharide was dissolved in a water/methanol mixture and 5 equivalents of 4-pentyn-1-amine were added. Reactions were performed for 48-96 h at room temperature with pH adjusted to 5.8 with acetate buffer. The samples were dialyzed and lyophilized. The aminated alginate was further modified by grafting of  $\beta$ -cyclodextrin (a starch macrocycle). The new polymer combined the gelation ability of alginate with the inclusion complex ability of cyclodextrins and has potential for application in controlled drug release (172).

Reductive amination of alginate was also performed on alginate oxidized with periodate using 4-(2-aminoethyl)-benzoic acid as the amine and picoline-borane as reducing agent with phosphate buffer (pH=6). The resulting alginate derivative can form a hydrogel for pH-controlled drug release (173).

Dextran was aminated with spermine, a polyamine. A solution of oxidized polysaccharide was added to a borate buffer solution (pH=11) containing 1.5 equivalents of polyamine. After 24 h of stirring at room temperature, excess sodium borohydride was added to reduce the imine that formed, during 24 h. After dialysis and lyophilization, amine-based conjugates were obtained with a 50% yield. The polymer was used in the preparation of nanoparticles as a vector of siRNA for gene silencing with application in colorectal cancer treatment (174).

This reaction can be used to synthesize polymers with primary amino groups if ammonia is used instead of an organic amine, creating cationic polysaccharides comparable with chitosan. This technique was applied to cellulose after its oxidation with periodate. Cellulose dialdehyde (1 g) reacted with an ammonium hydroxide solution (50 mL, 37% ammonia) at 50 °C protected from light for 3 h and using sodium cyanoborohydride (1:1 mass ratio to polymer) dissolved in ethanol as the reducing agent. After 18 h of reaction at 100 °C under reflux, the product was dried, redissolved, dialyzed and lyophilized. This novel cationic polymer showed better pH-independent hydration and better mucoadhesive properties than chitosan (175).

Polysaccharides carrying primary amino groups were also made from starch dialdehyde (1 g), and reductive amination was performed with an ammonium hydroxide solution (50 mL, 32% ammonia) at 50 °C protected from light for 3 h and using sodium cyanoborohydride (1:1 weight ratio to polymer) dissolved in ethanol as the reducing

agent. After 3 days, the aminated starch was purified by solvent evaporation, dialysis and lyophilization. The novel cationic polysaccharide showed superior mucoadhesive properties and less cytotoxic effect than chitosan (176).

### 1.3.3 Alkylation with ammonium quaternary salts

Another pathway to the introduction of amino groups in polysaccharides is through alkylation with trimethylammonium compounds, commonly used for obtaining quaternary ammonium derivatives of polysaccharides (Figure 1.16).

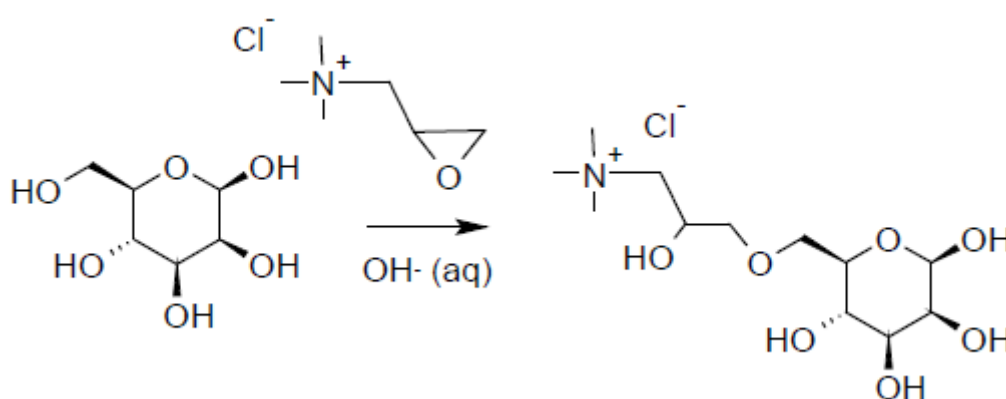


Figure 1.16: Alkylation of  $\beta$ -D-mannopyranose with glycidyltrimethylammonium chloride.

Chitosan, dissolved in alkaline aqueous medium, at 80 °C, was alkylated with glycidyltrimethylammonium chloride, which was added 3 times with 2 h intervals, totaling 3 equivalents. The product was isolated, dialyzed and lyophilized. The quaternary ammonium chitosan salt had a degree of alkylation of 90%. This modification improved water solubility in the whole pH range. Cytotoxicity increased with alkylation, but so did its efficacy as a transfection vector (177).

Curdlan was also cationized by alkylation, using different alkylating agents, either glycidyltrimethylammonium chloride or 3-chloro-2-hydroxypropyltrimethylammonium chloride. Curdlan was dissolved in a 0.5 M sodium hydroxide solution and the quaternization agent was added dropwise under constant stirring, with reaction times ranging from 4 to 6 h and temperatures ranging from 50 to 70 °C. The modified curdlan was precipitated, redissolved in water, neutralized, purified by diafiltration and lyophilized. The cationic curdlan synthesis was more successful with glycidyltrimethylammonium. Cationic curdlan was conjugated with anionic curdlan,

forming curdlan nanoparticles through polyelectrolyte complexation that could be used as drug carriers (178).

Pullulan was alkylated with glycidyltrimethylammonium (27 equivalents) in an aqueous solution of KOH (9 equivalents). The reaction took 24 h at 60 °C. After dilution, neutralization, dialysis and lyophilization, the quaternary ammonium pullulan was obtained. This polysaccharide was used for the preparation of pullulan-based nanoparticles by polyelectrolyte complexation, along with sulfated pullulan. These particles presented adequate characteristics for drug delivery applications and were able to associate bovine serum albumin (145).

Locust bean gum was similarly alkylated with glycidyltrimethylammonium in a potassium hydroxide solution. Glycidyltrimethylammonium was added twice, after 5 h and later after 24 h. The mixture was neutralized, dialyzed and dried. Using polyelectrolyte complexation, this cationic derivative was combined with an anionic locust bean gum derivative to produce nanoparticles with adequate properties for drug delivery applications (74).

#### 1.3.4 Carboxymethylation

Carboxymethylation is one of the most well-known polysaccharide modifications since the preparation of CMC. The reaction is usually carried out in an alkaline solution, using monochloroacetic acid or its sodium salt for introduction of carboxymethyl groups in polysaccharides (Figure 1.17) (179). Recently, more unconventional polysaccharides have been carboxymethylated for biomedical applications.

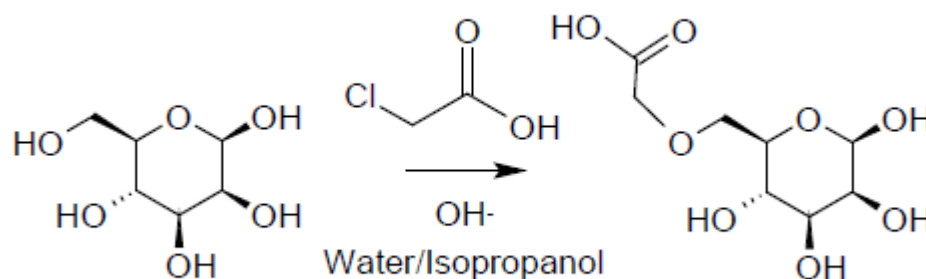


Figure 1.17: Carboxymethylation of  $\beta$ -D-mannopyranose with chloroacetic acid.

To modify curdlan, the reaction was performed in a suspension of isopropanol/water with sodium hydroxide and 3 additions, at 10 min intervals, of monochloroacetic acid, with the reaction taking 5 h at 55 °C. After filtration, washing, dialysis and lyophilization, the product was coupled with cholesterol by EDC/NHS-mediated ester formation. This compound was used as a nanoparticle carrier system for epirubicin. Results showed that the carrier prolonged the drug retention time in the plasma circulation, modified its biodistribution and enhanced its efficacy, while reducing its toxicity (84).

Carrageenan was carboxymethylated in variable conditions, suspended in an isopropanol-containing sodium hydroxide aqueous solution and using monochloroacetic acid as reagent. The modified carrageenan was recovered through vacuum filtration, washed and dried. This derivative displayed pH-dependent swelling and encapsulation efficiency, providing an alternative approach for oral delivery of macromolecules to the intestinal tract (180).

Carboxymethyl groups have also been added to starch. The reaction was done in an isopropanol/water mixture with sodium hydroxide and monochloroacetic acid, heated to 60 °C for 2 hours. After washing and drying, carboxymethyl starch with a degree of substitution of 49% was obtained. Along with chitosan, this starch derivative was used to produce nanoparticles to be loaded with 5-aminosalicylic acid, for drug delivery to the colon (181).

N,O-carboxymethyl chitosan was obtained by a similar procedure, with sodium hydroxide added in 5 instances, in 5 min intervals, to the isopropanol and polymer mixture, and monochloroacetic acid added in 5 portions over 20 min. After 3 h at 60 °C, the mixture was filtered and the product washed and dried. This derivative was crosslinked with hyaluronic acid oxidized with periodate, forming an hydrogel that was successful in preventing post-operative peritoneal adhesions, as demonstrated in a rat model (162).

Carboxymethyl pullulan was also synthesized. Pullulan and sodium borohydride were dissolved in water, to which sodium hydroxide and monochloroacetic acid were added in 3 steps, initially, after 1 h and after 30 min, with a total reaction time of 18 h at 70 °C. Carboxymethylpullulan with a degree of substitution of 70% was recovered after

dialysis by lyophilization. Interpenetrating this pullulan derivative with poly(N-isopropylacrylamide), a temperature-sensitive polymer, was achieved by crosslinking with N,N'-methylenebisacrylamide, creating a thermo and pH-sensitive hydrogel for drug delivery applications (182).

Locust bean gum has also been carboxymethylated. The gum was kneaded with an ice-cold sodium hydroxide solution and a variable amount of a chloroacetic acid solution was added over 1 h at 15 °C. Then the semisolid mass was heated to 65 °C and left to react for 1 h more. The modified polymer was washed, dialyzed and dried. Poly(vinyl alcohol) was utilized along with the carboxymethyl locust bean gum to prepare interpenetrating polymer network microspheres of buflomedil hydrochloride for controlled drug delivery, and *in vitro* tests showed retarded drug release up to 12 h (183).

### 1.3.5 Sulfation

Sulfated glycosaminoglycans have versatile biological activities and are also interesting as drug delivery materials. Therefore, the introduction of sulfate groups in other polysaccharides is a technique used to obtain new derivatives that mimic those properties. This can be achieved with different sulfating agents, such as sulfuric acid, sulfur trioxide or chlorosulfonic acid in dimethylformamide (DMF) (Figure 1.18) (184).

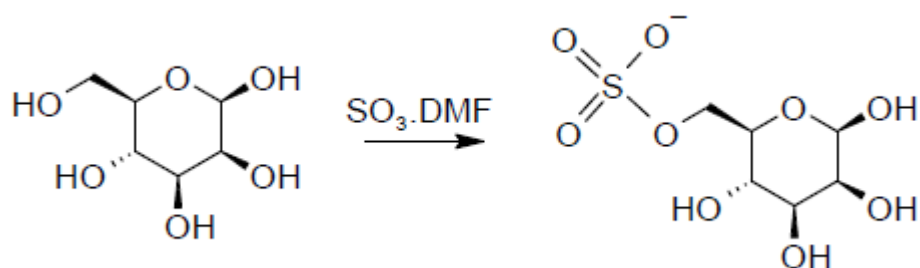


Figure 1.18: Sulfation of  $\beta$ -D-mannopyranose with  $SO_3$ -DMF.

Chitosan was sulfated using a mixture of sulfuric acid and chlorosulfonic acid cooled to 0-4 °C, then warmed to room temperature and stirred for 30 min. The derivative was precipitated in cold diethyl ether, dissolved in water, neutralized, dialysed and lyophilized. Later, the polysaccharide was coupled with 3-O-hemisuccinate glycyrrhetic acid by EDC/NHS-mediated amide formation, which served as both a

hydrophobic group and a liver-targeting ligand. This new compound was used to prepare micelles loaded with doxorubicin, which showed potential as a liver-cancer targeting carrier (185).

Sulfated pullulan was prepared by dispersing pullulan in dimethylformamide DMF and adding sulfur trioxide/DMF complex. The reaction took 4 h at 60 °C. The mixture was cooled and neutralized and the solvent was evaporated. The product was dissolved in water for dialysis, and then lyophilized. This derivative was used for the preparation of pullulan-based nanoparticles by polyelectrolyte complexation, along with quaternary ammonium pullulan (145).

A sulfated derivative of locust bean gum was similarly prepared. This polymer was successfully used to produce nanoparticles by polyelectrolyte complexation with two cationic polysaccharides (chitosan and a quaternary ammonium locust bean gum derivative) with adequate properties for drug delivery applications (74).

### 1.3.6 Phosphorylation

Phosphorylation of polysaccharides consists in the substitution of hydroxyl groups of the carbohydrates by phosphate or phosphonate groups. This can be achieved with different methods, such as using phosphorous acid (Figure 1.19), resulting in a phosphonate, or phosphorus pentoxide yielding a phosphate (186).

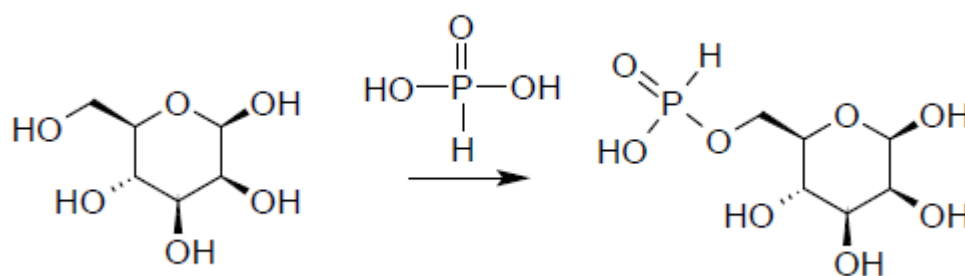


Figure 1.19: Phosphorylation of  $\beta$ -D-mannopyranose with phosphorous acid.

Curdlan was modified to have phosphonate groups by reaction with phosphorous acid in molten urea at 145 °C for 3 to 5 h. After cooling, the mixture is dissolved in a sodium hydroxide solution and precipitated in methanol various times to purify the product, then redissolved, diafiltrated and recovered by lyophilization (187). This

polysaccharide was used in the preparation of nanoparticles with cationic curdlan (178) and crosslinked with epichlorohydrin to form anionic microgels for controlled drug release of cationic drugs (85).

Starch and its derivative hydroxypropyl starch were phosphorylated using phosphorus pentoxide mixed in water. The reaction was done at room temperature for 1 h and then the mixture was dialysed and dried. These modified starches were loaded into self-emulsifying drug delivery systems, which optimized mucus diffusion properties, due to a zeta potential shift to positive. This strategy may increase bioavailability of drugs administered via mucosal membranes (188).

Chitosan was phosphorylated by dissolution in an acetic acid solution, heated to 70 °C, to which a phosphorous acid solution and a formaldehyde solution were added. After 3 h of reaction, the mixture was cooled and ethanol added to precipitate the polymer, which was then washed, dialyzed and lyophilized. The phosphorylated chitosan was used as a base for a hydrogel containing ovalbumin as a vaccine delivery system that induced antigen-specific immune response when injected in test mice (189).

## 2 Objectives

This work aims at chemically modifying a polysaccharide from the seeds of a native plant, the locust bean gum, and to create and characterize a cationic polymer, through different synthesis pathways. This polymer of added value will then be used in the production of nanoparticles with carrageenan, much like chitosan is usually employed, in different mass ratios to obtain nanoparticles with suitable properties for drug delivery.

## 3 Materials and methods

### 3.1 Materials

Locust bean gum (LBG) was gifted by Industrial Fareense (Faro, Portugal). Potassium bromide (KBr), silver nitrate ( $\text{AgNO}_3$ ) sodium periodate, Oxone<sup>®</sup>, monopersulfate compound, sodium borohydride, 2,2,6,6-tetramethylpiperidin-1-yloxy radical (TEMPO) were obtained from Sigma-Aldrich (USA). K-Carrageenan (CRG) and iron (II) sulfate heptahydrate ( $\text{FeSO}_4 \cdot 7\text{H}_2\text{O}$ ) from Fluka (Denmark); sodium hypochlorite from Honeywell (USA); hydrochloric acid 37% from VWR (USA); ammonium persulfate from Riedel-de Haën (Germany); sodium bromide and piperidine from Merck (Germany); ammonium chloride, from José Manuel Gomes dos Santos, Lda (Portugal).

Ultrapure water was obtained from Mili-Q plus, Milipore (Portugal) and ethanol was from Álcool e Géneros Alimentares, S.A. (Portugal).

Dialysis was performed using SnakeSkin<sup>™</sup> Dialysis Tubing (Pierce, USA) and lyophilization was performed on a Labconco<sup>®</sup> FreeZone 6 Liter Benchtop Freeze Dry System freeze dryer.

Reactions were followed with a Thermo Evolution 300 UV-Vis Spectrophotometer.

FTIR spectra were acquired using Bruker Tensor 27. Samples were ground in a mortar and pestle with KBr and compressed into disks. The spectra were obtained by collecting 32-scan interferograms in transmittance mode with  $4\text{ cm}^{-1}$  resolution in the  $4000\text{-}400\text{ cm}^{-1}$  region.

Nuclear magnetic resonance was performed on a 500 MHz Jeol spectrometer.

Nanoparticles size and PDI were measured by dynamic light scattering and zeta potential was measured by laser Doppler anemometry using a Zetasizer Nano ZS (Malvern instruments, UK).

### 3.2 Synthesis of LBG derivatives

#### 3.2.1 Purification of LBG

Purification of LBG is necessary to remove the protein content (3 to 7 %) that is usually present in commercial samples (131). The procedure consisted in wetting 5.0 g of LBG with ethanol and adding distilled water, preheated to  $85\text{ }^\circ\text{C}$ , and stirring for 1 h. After this, the dispersion was cooled to room temperature and subsequently centrifuged ( $22,000 \times g$ ,  $20\text{ }^\circ\text{C}$ , 1 h). The supernatant (LBG solution free of protein) was added to an

equal volume of ethanol to precipitate the LBG. After vacuum filtration, the precipitate was finally dried in a vacuum oven at 30 °C during 72 h. The purified product was a white powder, weighting 3.3 g, which was ground and stored until necessary.

### 3.2.2 Oxidation

#### 3.2.2.1 Oxidation with periodate

Oxidation of LBG was performed by an adaptation of a described procedure (190). Purified LBG (2 g) was dispersed in distilled water (180 mL) previously heated to 65 °C and stirred for 24 h at room temperature. Sodium periodate was added to the solution and the mixture allowed to react for 6 h to 26 h, at room temperature, protected from light. The mixture was then dialyzed for 72 h against water, with the dialysis medium being changed twice a day. The presence of iodate in the dialysis medium was tested by the silver nitrate precipitation essay. After dialysis, the mixture was frozen to -80 °C and lyophilized. The resulting products, periodate oxidized LBG i), ii) and iii) were a white, fibrous, cotton-like material. The different sets of conditions were:

- i) Two equivalents of sodium periodate were used (1.06 g). The reaction mixture was divided in two vessels, letting one of them react for 6 h and the other for 26 h. The obtained masses were 0.743 g and 0.931 g, corresponding to the 6 h and 26 h reactions.
- ii) Four equivalents of sodium periodate were used (2.11 g). The reaction mixture was divided in two vessels, letting one of them react for 4 h and the other for 6 h. The obtained masses were 0.801 g after the 4 h reaction plus 0.830 g after the 6 h reaction.  
IR (KBr): 1712  $\text{cm}^{-1}$  (C=O).
- iii) Eight equivalents of sodium periodate were used (4.22 g). The mixture reacted for 6 h. Finally, the product weighted 1.675 g.  
IR (KBr): 1718  $\text{cm}^{-1}$  (C=O).

#### 3.2.2.2 Oxidation with TEMPO

Oxidation of LBG was performed using TEMPO as the oxidizing agent, following the method described by Braz *et al.*, (74) for oxidizing LBG's primary alcohols to

carboxyl groups, but using half the oxidizing agent, in order to stop the oxidation at the carbonyl stage.

Purified LBG (500 mg) was dispersed in distilled water (200 mL) heated to 80 °C for 30 min. After 30 min, the mixture was left to cool until room temperature. Water was added to complete 200 mL, replenishing the water that evaporated, and the mixture was cooled in an iced water bath. Then  $2.6 \times 10^{-3}$  equivalents of TEMPO (10 mg) and  $1.9 \times 10^{-2}$  equivalents of NaBr (50 mg) were added, while stirring. A 15% sodium hypochlorite solution (1.5 mL) with pH adjusted to 9.3 with HCl (2 M) solution, was mixed with the reaction mixture. The pH was kept at 9.3 during 4 h by the addition of NaOH (0.05 M) when necessary. The mixture was then dialyzed for 72 h against water, with the dialysis medium being changed twice a day. After dialysis, the mixture was frozen to -80 °C and lyophilized. The resulting product weighted 0.380 g and was a gray, fibrous, cotton-like material.

IR (KBr):  $1730 \text{ cm}^{-1}$  (C=O)

### 3.2.2.3 Oxidation with Oxone<sup>®</sup>

Oxidation of LBG was performed using Oxone<sup>®</sup> as oxidizing agent, in the presence of manganese sulfate, adapting the procedure of Sánchez *et al.* (191).

Purified LBG (2 g) was wetted with ethanol and distilled water (180 mL), previously heated to 65 °C, was added. The mixture was kept at 65 °C for 1 h and then left to cool until room temperature and stirred for 48 h, until mostly dissolved. Then, 1 equivalent of Oxone<sup>®</sup> (3.04 g) and 1 equivalent of manganese sulfate (1.70 g) were added. The reaction was monitored by UV-Vis spectrophotometry (aliquots transferred to a quartz cuvette and scanned from 190 to 900 nm) to verify that the reaction was complete, at 9 h. The mixture was then dialyzed for 72 h against water, with the dialysis medium being changed twice a day. After dialysis, the mixture was concentrated under reduced pressure at 60 °C, precipitated in ethanol and centrifuged ( $22\,000 \times g$ , 20 min). The precipitate was left to dry for 48 h and further dried in a vacuum oven at 40 °C for 1 day, affording 1.792 g of light gray solid that was grinded and stored until further use.

IR (KBr):  $1730 \text{ cm}^{-1}$  (C=O)

#### 3.2.2.4 Oxidation with ammonium persulfate

Oxidation of LBG was performed using ammonium persulfate as the oxidizing agent and iron (II) sulfate heptahydrate as catalyst. This kind of reaction was proven effective by Rodriguez *et al.* (192).

Purified LBG (500 mg) was dispersed in distilled water (200 mL) heated to 80 °C for 30 min, after which the mixture was left to cool until room temperature. After cooled, one equivalent of ammonium persulfate (0.563 g) and  $4.9 \times 10^{-3}$  equivalents of iron (II) sulfate heptahydrate (0.034 g) were added under stirring. After 4 h of reaction, the mixture was then dialyzed for 72 h against water, with the dialysis medium being changed twice a day. After dialysis, the mixture was frozen to -80 °C and lyophilized. The resulting product weighed 0.335 g and was a gray, fibrous, cotton-like material.

IR (KBr):  $1740 \text{ cm}^{-1}$  (C=O)

#### 3.2.3 Reductive amination

##### 3.2.3.1 Reductive amination of periodate oxidized LBG

Reductive amination of the oxidized polymer was performed according to a procedure described by Bergman *et al.* (193).

Oxidized LBG was humidified with ethanol. Then, ammonium chloride was added to the reaction flask, along with piperidine. The mixture was then heated to 75 °C in an oil bath under stirring and protected from moisture. The following sets of conditions for periodate oxidized LBG were tried:

- i) 500 mg of oxidized LBG, 1 equivalent of ammonium chloride (133 mg) and 1 equivalent of piperidine (245  $\mu\text{L}$ ) and 24 h of reaction time;
- ii) 500 mg of oxidized LBG, 2 equivalents of ammonium chloride (270 mg) and 2 equivalents of piperidine (490  $\mu\text{L}$ ) and 24 h of reaction time;
- iii) 500 mg of oxidized LBG, 1 equivalent of ammonium chloride (133 mg) and 1 equivalent of piperidine (245  $\mu\text{L}$ ) and follow up of carbonyl disappearance by FTIR spectroscopy (air dried aliquots pressed in KBr disks), which was complete after 5 h of reaction.

After the imine was formed, distilled water heated to 85 °C was added to the reaction flask to dissolve it and the solution was left to cool down to room temperature.

Then, sodium borohydride was added, to reduce the imine. The different sets of conditions were:

- i) 4 equivalents of sodium borohydride (375 mg) were added and the reaction mixture stirred overnight; after heating to 50 °C in an oil bath for 4.5 h, the mixture was left to cool down before the addition of 4 more equivalents of sodium borohydride. After the addition, the mixture was reheated and left to react overnight.
- ii) 8 equivalents of sodium borohydride (750 mg) were added and the mixture was heated at 50 °C overnight. Then, another 8 equivalents were added, 4 at a time in two different instants, 18 and 20 h after the initial addition, and left to react overnight.
- iii) 4.3 equivalents of sodium borohydride (400 mg) were added and the mixture was heated to 50 °C. The reaction was monitored by UV-Vis spectrophotometry at 30 min intervals (aliquots transferred to a quartz cuvette and scanned from 250 to 700 nm) until completion, at 2 h.

Finally, the mixture was dialyzed against distilled water (method i) or pH 4 hydrochloric acid solution (methods ii and iii) for 72 h, with the dialysis medium being changed twice a day. After dialysis, the mixture was frozen to -80 °C and lyophilized. After lyophilization and grinding, amino LBG (ALBG) was obtained as a brownish powder. The masses of product obtained were i) 0.135 g, ii) 0.168 g and iii) 0.104 g.

ii) IR (KBr): 1060  $\text{cm}^{-1}$  (C-N)

$^1\text{H-NMR}$  ( $\text{D}_2\text{O}$ ),  $\delta$  (ppm): 3.380 (-CH-CH<sub>2</sub>-, dd,  $J_1 = 12$  Hz,  $J_2 = 6.5$  Hz); 3.474 (-CH- + -CH<sub>2</sub>-, m); 3.539 (-CH-,d); 3.3562 (-CH- + -CH<sub>2</sub>-, m); 3.605 (-CH-, tt,  $J_1 = 7$  Hz,  $J_2 = 4$  Hz).

iii) IR (KBr): 1718  $\text{cm}^{-1}$  (C=O)

### 3.2.3.2 Reductive amination of TEMPO oxidized LBG

Reductive amination was performed on the TEMPO oxidized polymer, in the following conditions: 0.348 g of oxidized LBG, 1 equivalent of ammonium chloride (92.4 mg) and 1 equivalent of piperidine (171  $\mu\text{L}$ ), and 5 h of reaction time. Distilled water heated to 85 °C was added to the reaction flask to dissolve the polymer and the solution

was left to cool down to room temperature. Four equivalents of sodium borohydride (230 mg) were added and the mixture was heated to 50 °C. The reaction was monitored by UV-Vis spectrophotometry at 30 min intervals (aliquots transferred to a quartz cuvette and scanned from 250 to 700 nm) until completion, at 3 h.

Finally, the mixture was neutralized with hydrochloric acid and dialyzed against pH 4 hydrochloric acid solution for 72 h, with the dialysis medium being changed twice a day. After dialysis, the mixture's solvent was evaporated, leaving behind a film of polymer that was collected and dried in a vacuum oven at 40 °C for 1 day. ALBG was obtained as a yellow powder. The mass of product obtained was 0.250 g.

IR (KBr): 1730  $\text{cm}^{-1}$  (COOH)

IR (KBr): 1090  $\text{cm}^{-1}$  (C-N)

### 3.2.3.3 Reductive amination of Oxone<sup>®</sup> oxidized LBG

Reductive amination was performed on the Oxone<sup>®</sup> oxidized polymer, in the following conditions: 1.55 g of oxidized LBG, 1 equivalent of ammonium chloride (411 mg) and 1 equivalent of piperidine (760  $\mu\text{L}$ ). Follow up of carbonyl disappearance was performed by FTIR spectroscopy (air dried aliquots pressed in KBr disks), which was complete after 4 h of reaction. Ethanol was added to the reaction flask and the solution was left to cool down to room temperature. Four equivalents of sodium borohydride (1.164 mg) were added and the mixture was heated to 50 °C. The reaction was monitored by UV-Vis spectrophotometry at 30 min intervals (aliquots transferred to a quartz cuvette and scanned from 190 to 900 nm) until completion, at 4 h. The ethanol was evaporated under reduced pressure and water heated to 80 °C was added to the reaction flask. As some sodium borohydride still had not dissolved, the reaction continued, as seen by the release of gas bubbles. Therefore, the mixture was left to react 1 h more. Then, the mixture was neutralized with hydrochloric acid and dialyzed against pH 4 hydrochloric acid solution for 72 h, with the dialysis medium being changed twice a day. After dialysis, the mixture was concentrated under reduced pressure at 60 °C, precipitated in ethanol and centrifuged (22 000  $\times$  g, 20 min). The precipitate was left to dry for 48 h and further dried in a in a vacuum oven at 40 °C for 1 day, affording 1.101 g of gray solid that was grinded and stored until further use.

IR (KBr): 1085  $\text{cm}^{-1}$  (C-N)

#### 3.2.3.4 Reductive amination of ammonium persulfate oxidized LBG

Reductive amination was performed on the ammonium persulfate oxidized polymer, in the following conditions: 0.240 g of oxidized LBG, 1 equivalent of ammonium chloride (64.2 mg) and 1 equivalent of piperidine (119  $\mu\text{L}$ ). Follow up of carbonyl disappearance was performed by FTIR spectroscopy (air dried aliquots pressed in KBr disks), which was complete after 5 h of reaction. Distilled water heated to 85  $^{\circ}\text{C}$  was added to the reaction flask to dissolve the polymer and the solution was left to cool down to room temperature. Four equivalents of sodium borohydride (192 mg) were added and the mixture was heated to 50  $^{\circ}\text{C}$ . The reaction was monitored by UV-Vis spectrophotometry at 30 min intervals (aliquots transferred to a quartz cuvette and scanned from 250 to 700 nm) until completion, at 2 h.

At last, the mixture was neutralized with hydrochloric acid and dialyzed against pH 4 hydrochloric acid solution for 72 h, with the dialysis medium being changed twice a day. After dialysis, the mixture's solvent was evaporated, leaving behind a brown gum that was collected and left to air dry at room temperature. As the yield was very low, the product was not enough for characterization nor nanoparticle production, and was discarded.

### 3.3 Production of ALBG/CRG nanoparticles

Nanoparticles were prepared by polyelectrolyte complexation as *per* Braz *et al.* (30) using mass ratios of ALBG to CRG from 4/1 to 1/4. To prepare the particles, 0.8 mL of one polymer solution, diluted from the stock solution to different concentrations, was added to 2 mL of the other polymer stock solution (Figure 3.1). The resulting mixture is gently stirred for 10 min, after which the particles, which formed instantaneously, are ready for analysis.

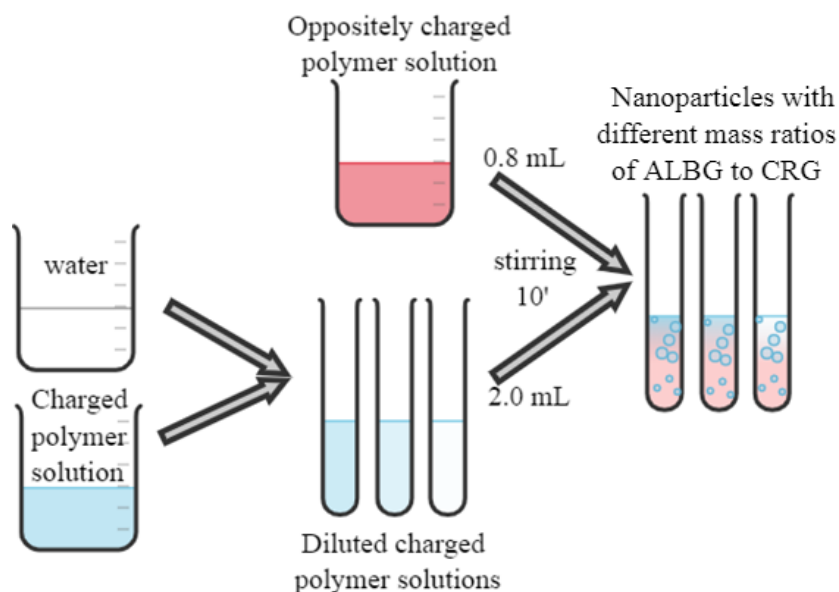


Figure 3.1: Nanoparticle production procedure scheme.

To allow for various mass ratios while keeping the same method and volumes, two different pairs of stock solution were prepared. The first pair, used to make particles with a higher ratio of ALBG, consisted of a 1 mg/mL ALBG solution, to be used directly and a 2 mg/mL CRG solution, to be diluted before use. On the other hand, for particles with a higher ratio of CRG, the solutions were a 1 mg/mL ALBG solution and a 2.5 mg/mL CRG solution to be diluted before use.

The stock solutions were prepared using ultrapure water, heated to 60 °C, stirred for 1 h and filtered with a 0.45  $\mu\text{m}$  filter before use.

### 3.4 Characterization of ALBG/CRG nanoparticles

Determination of the nanoparticles size, zeta potential and polydispersity index (PDI) were performed immediately after preparation. Samples consisted of 40  $\mu\text{L}$  of nanoparticles solution diluted in 1 mL of ultrapure water.

## 4 Results and discussion

### 4.1 Synthesis and characterization of locust bean gum derivatives

#### 4.1.1 Oxidation of LBG

Oxidation employing periodate results in the double oxidation of a *cis*-diol, and also, to a lower extent, of an equatorial *trans*-diol, to two aldehydes and cleavage of the carbon-carbon bond between the carbons bearing the hydroxyl groups (190), as shown in Figure 4.1.

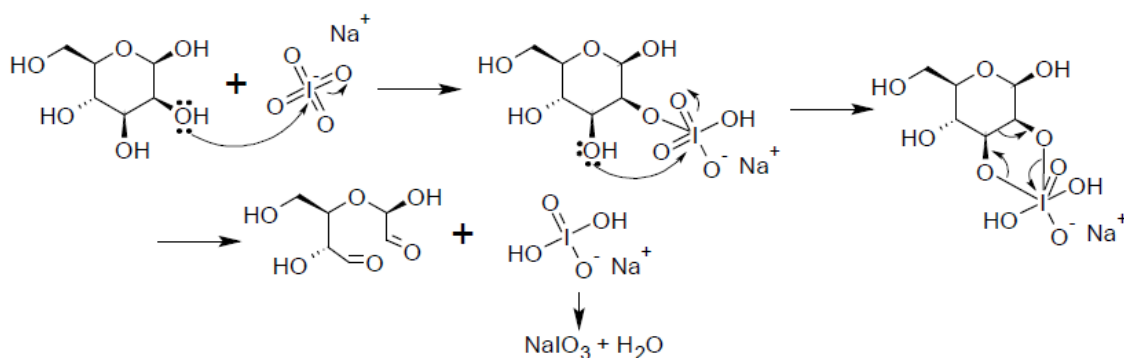


Figure 4.1: Mechanism of periodate diol cleavage.

Oxidation was performed using different quantities of periodate (2, 4 and 8 equivalents) and different reaction times (4, 6 and 26 h) were also tried, with the goal of oxidizing two *cis*-diols per structural unit, ending up with 4 aldehydes. This would afford, in the final product, a degree of substitution near 80 mol%, similar to that found in commercial chitosan.

FTIR spectroscopy analysis confirmed the presence of aldehyde groups in the products obtained in all reaction conditions tested, by the appearance of the aldehyde C=O stretching band at  $1712\text{ cm}^{-1}$ , shown in Figure 4.2 a).

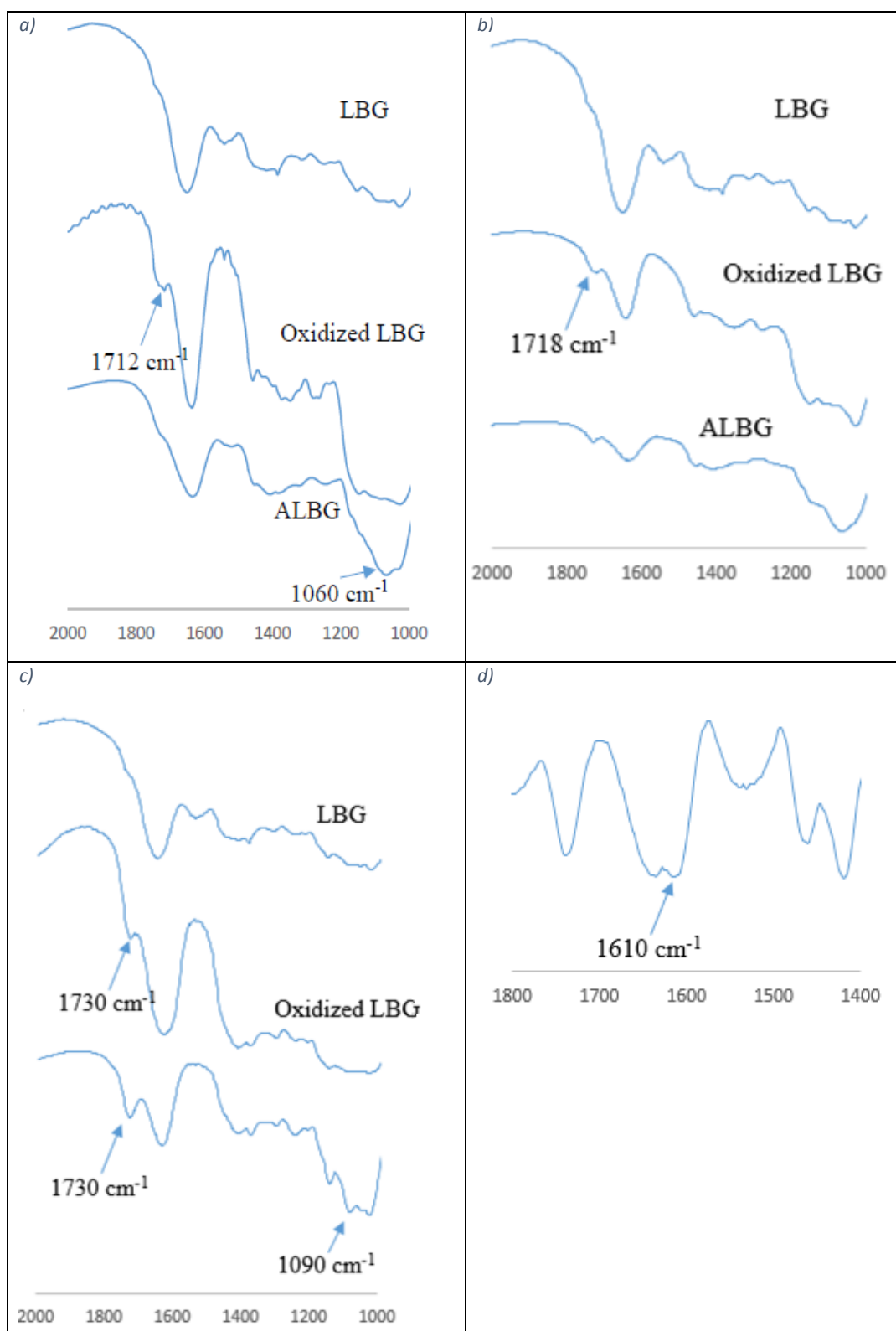


Figure 4.2: a) FTIR spectra of LBG, LBG oxidized with 4 equivalents of periodate and ALBG. Arrows indicate the carbonyl band in oxidized LBG and that of C-N in ALBG. b) FTIR spectra of LBG, LBG oxidized with 8 equivalents of periodate and ALBG. Arrow indicates the carbonyl band in oxidized LBG. c) FTIR spectra of LBG, LBG oxidized with TEMPO and ALBG. Arrows indicate the carbonyl band in oxidized LBG and that of carboxylic acid and C-N in ALBG. d) Second derivative of the FTIR spectrum of LBG oxidized with TEMPO. The arrow points the carboxylate band. e) FTIR spectra of LBG, LBG oxidized with Oxone<sup>®</sup> and ALBG. Arrows indicate the carbonyl band in oxidized LBG and that of C-N in ALBG. f) FTIR spectra of LBG and ammonium persulfate oxidized LBG. Arrow indicates the carbonyl band in oxidized LBG.

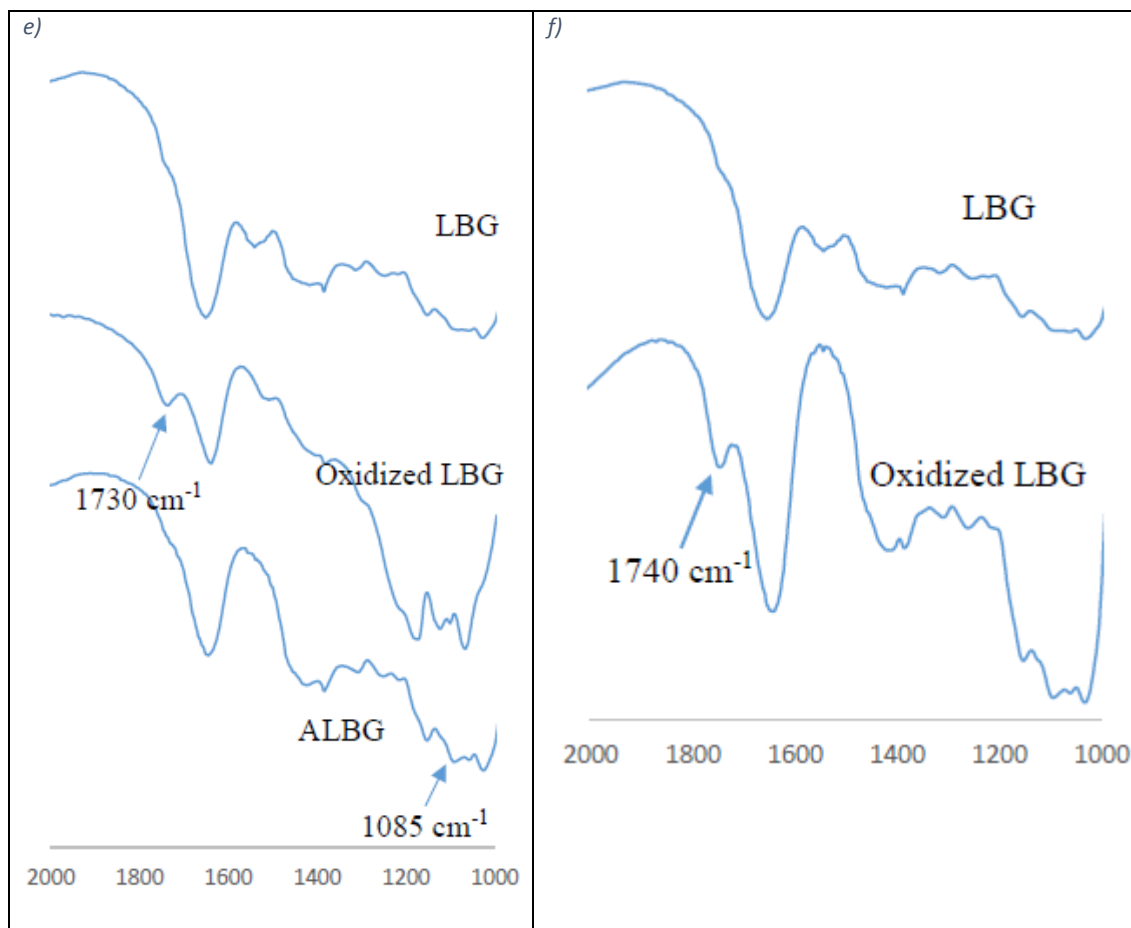


Figure 4.2 (continued)

From the relative intensity of this band, it appears that the different samples have different quantities of aldehyde groups, with the sample obtained by reaction with 8 equivalents of periodate Figure 4.2 b) showing the highest amount, while the sample obtained by reaction with 2 equivalents (data not shown) showed the lowest. The different reaction times in the same reaction conditions seemed to lead to similar band intensities, therefore those products were deemed equal and combined.

Reaction of galactomannans with TEMPO has been shown to result in oxidation of C-6 (194), yielding mostly carboxyl groups, as represented in Figure 1.13. To investigate if the reaction could produce a polysaccharide that was only once oxidized, resulting in aldehyde groups instead of carboxyl, the procedure described in reference (74) was repeated, using only half the amount of reagents to the same quantity of polymer.

While the periodate reaction produced a polymer with a very different structure, due to cleavage of the carbon-carbon bond and breaking of the ring, oxidation of the primary alcohol at C-6 should preserve the polysaccharide original structure, as shown in

Figure 4.3. The amount of hypochlorite used was 1.2 equivalents per each of the four primary hydroxyl groups prone to oxidation, one belonging to the galactopyranosyl residue and the others to the unsubstituted mannopyranosyl units.

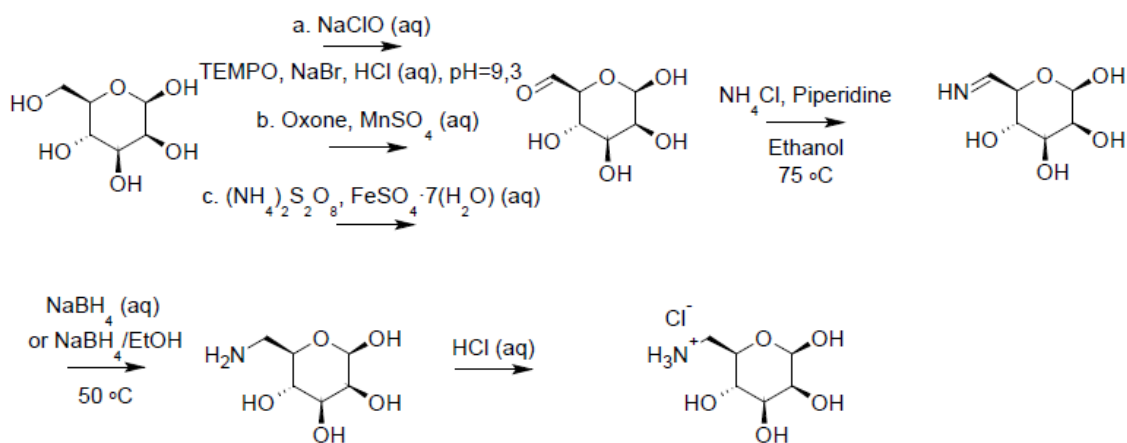


Figure 4.3: C-6 oxidation of a  $\beta$ -D-mannopyranose with a. TEMPO, b. Oxone<sup>®</sup>, c. ammonium persulfate, followed by reductive amination.

After FTIR spectroscopy analysis (Figure 4.2 c)), a band around  $1730\text{ cm}^{-1}$  could be observed, which could be attributed to the presence of an aldehyde group. Based on the observation of the second derivative of this spectra, in Figure 4.2 d), it seemed possible that there was oxidation to carboxylate, represented by the band at  $1610\text{ cm}^{-1}$  which is identifiable in the second derivative but overlapped by the adsorbed water band in the original spectrum.

Oxone<sup>®</sup> was also used as an oxidizing agent for LBG, in the presence of  $\text{MnSO}_4$ . Like TEMPO, its targets are primary alcohols (191), in this case the unsubstituted C-6 carbons, keeping the structure of LBG mostly intact, while theoretically providing 4 carbonyl groups per structural group. FTIR spectra analysis, in Figure 4.2 e), showed the presence of a band at  $1730\text{ cm}^{-1}$ , representative of a carbonyl group.

As Oxone<sup>®</sup> is a persulfate compound, a similar reaction was attempted using ammonium persulfate and iron (II) as catalyst. This reaction has already proven successful in obtaining carbonyl groups (192). In this case, FTIR spectra analysis, (Figure 4.2 f)), seems to confirm the presence of aldehyde in the sample, as a band around  $1740\text{ cm}^{-1}$  can be observed.

#### 4.1.2 Reductive amination of LBG

Reductive amination is a reaction between a carbonyl and an amino group, forming an imine, followed by reduction of the C=N bond by addition of a reducing agent (195), as shown in Figure 4.4.

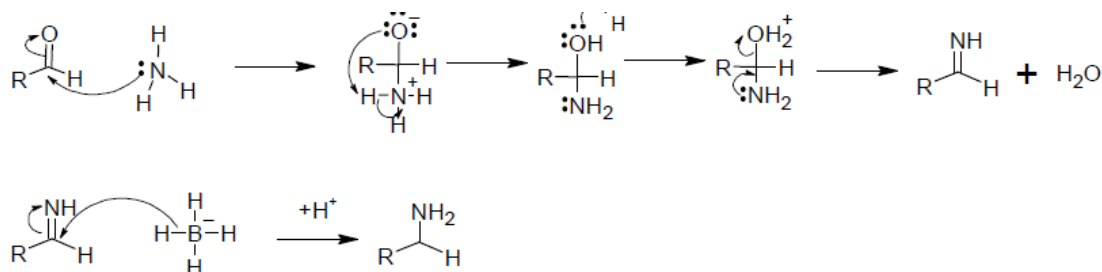


Figure 4.4: Reductive amination of an aldehyde group.

After oxidation of LBG, in order to obtain aldehyde groups, these were reacted with ammonium chloride, in the presence of piperidine, to form imines (193) that were subsequently reduced to primary amines by sodium borohydride (Figure 4.5). Dialysis against an acidic solution (pH=4) allowed to obtain the final product (ALBG) in the form of hydrochloride, in order to increase water solubility.

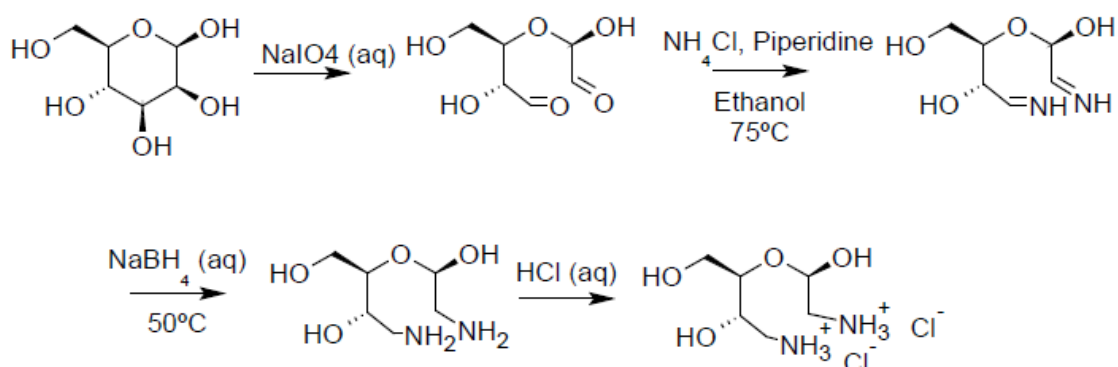


Figure 4.5: Oxidation by periodate and reductive amination of a  $\beta$ -D-mannopyranose.

Reductive amination of LBG oxidized with periodate was performed under different conditions. In the formation of the imine intermediate, different amounts (1 or 2 equivalents) of ammonium chloride were used and the time of reaction was also varied (5 or 24 h); for the reduction to amine, the reducing agent was varied between 4 and 16 equivalents and reaction time between 2 h and 2 days.

In the FTIR spectrum of the product, the bands relative to the amine, like the N-H stretch ( $3400\text{-}3380\text{ cm}^{-1}$ ), are impossible to identify, being covered by the polysaccharide hydroxyl groups. Meanwhile, the C-N stretch at  $1060\text{ cm}^{-1}$  can be observed, as marked in Figure 4.2

From the relative intensity of this band, it appears that the different samples have different quantities of amine groups, with the sample obtained by reaction of oxidized LBG (prepared using 4 equivalents of sodium periodate) with 2 equivalents of ammonium chloride for 24 h showing the highest degree of substitution, followed by the reaction of oxidized LBG (prepared with 8 equivalents of periodate) with 1 equivalent of ammonium chloride for 5 h. The reaction of oxidized LBG (prepared with 2 equivalents of periodate) with 1 equivalent of ammonium chloride was the least successful, as expected by the lack of aldehyde groups observed. It was expected to obtain a better degree of substitution after performing the reductive amination in LBG oxidized with 8 equivalents of periodate, but this was not the case, and that ALBG spectra also preserved a peak at  $1718\text{ cm}^{-1}$ , which can correspond to aldehyde groups in the bulk undispersed gum that did not contact with the reagents. The unreliability of the different reactions can be attributed to the difficulty in obtaining a homogenous gum-ethanol dispersion for the reductive amination to take place, as well as an aqueous or ethanolic solution in the reduction step.

This reaction proved to be troublesome as its yield is very low. The reaction time was reduced from 24 to 5 h to avoid the polysaccharide hydrolysis, and reductive amination in ethanol instead of water was tested, but a better yield was not achieved.

Like the oxidation with periodate, every other oxidation reaction was followed by a reductive amination in order to obtain the desired primary amine groups. For reductive amination of TEMPO oxidized LBG, 1 equivalent of ammonium chloride was used to form the imine, for 5 h. Then the imine was reduced using 4 equivalents of sodium borohydride for 3 h. After dialysis, this product was isolated by solvent evaporation instead of lyophilization, which did not show any ill effect to the product.

After reductive amination, the band around  $1730\text{ cm}^{-1}$  was still present (Figure 4.2 c)). Considering aldehydes would either react with the ammonium chloride or be reduced by sodium borohydride back to alcohols, the band is possibly due to carboxylic acid groups, which would be stable enough to avoid reduction. Therefore, it is thought that some aldehyde groups were still present in the polysaccharide, which were aminated

resulting in the band around  $1090\text{ cm}^{-1}$ , but most of the oxidation resulted in carboxylate groups which, after aldehyde reduction and at a lower pH, could easily be identified in the ALBG spectrum. With 1.2 equivalents of hypochlorite per each of 4 hydroxyl groups, it was expected that 4 aldehyde groups were obtained. Instead, it appears that less hydroxyl groups were oxidized and some were twice oxidized, resulting in carboxyl groups.

On the reaction using Oxone<sup>®</sup> oxidized LBG, imine was also formed using 1 equivalent of ammonium chloride, which reacted for 4 h. Reduction was performed for 4 h in ethanol plus 1 h in water, with 4 equivalents of borohydride. This was the only assay where reduction was attempted in ethanol for most of the time, in order to tackle the low yield problem. The attempt did not prove useful, as reaction time had to be lengthened in ethanol and the final yield was similar. To isolate the product, the dialyzed solution was poured in ethanol to precipitate the product, centrifuged and the precipitate was dried. Observing the ALBG FTIR spectrum on Figure 4.2 e), the new band at  $1085\text{ cm}^{-1}$  can represent the C-N stretch, therefore some amine groups are expected to be present in this compound.

Regarding the reductive amination of LBG oxidized with ammonium persulfate, the product isolated was too little to collect, therefore no FTIR spectrum was acquired.

On all the performed reactions, one obstacle was the preparation of a homogenous reaction media, either a solution or a uniform suspension. Dissolution of the polymer was impossible to achieve completely, and the remaining solid polymer regularly formed dense materials, making it harder for the core of the polysaccharide to contact with the reagents. In the future, a pretreatment of the polymer, like a partial hydrolysis (196) or the use of salts (175), to make it easier to work with, could help overcome this difficulty.

The ALBG sample obtained by reductive amination of the LBG oxidized with 4 equivalents of periodate was also analyzed using <sup>1</sup>H and HSQC spectroscopy. The obtained results are shown in Figure 4.6.

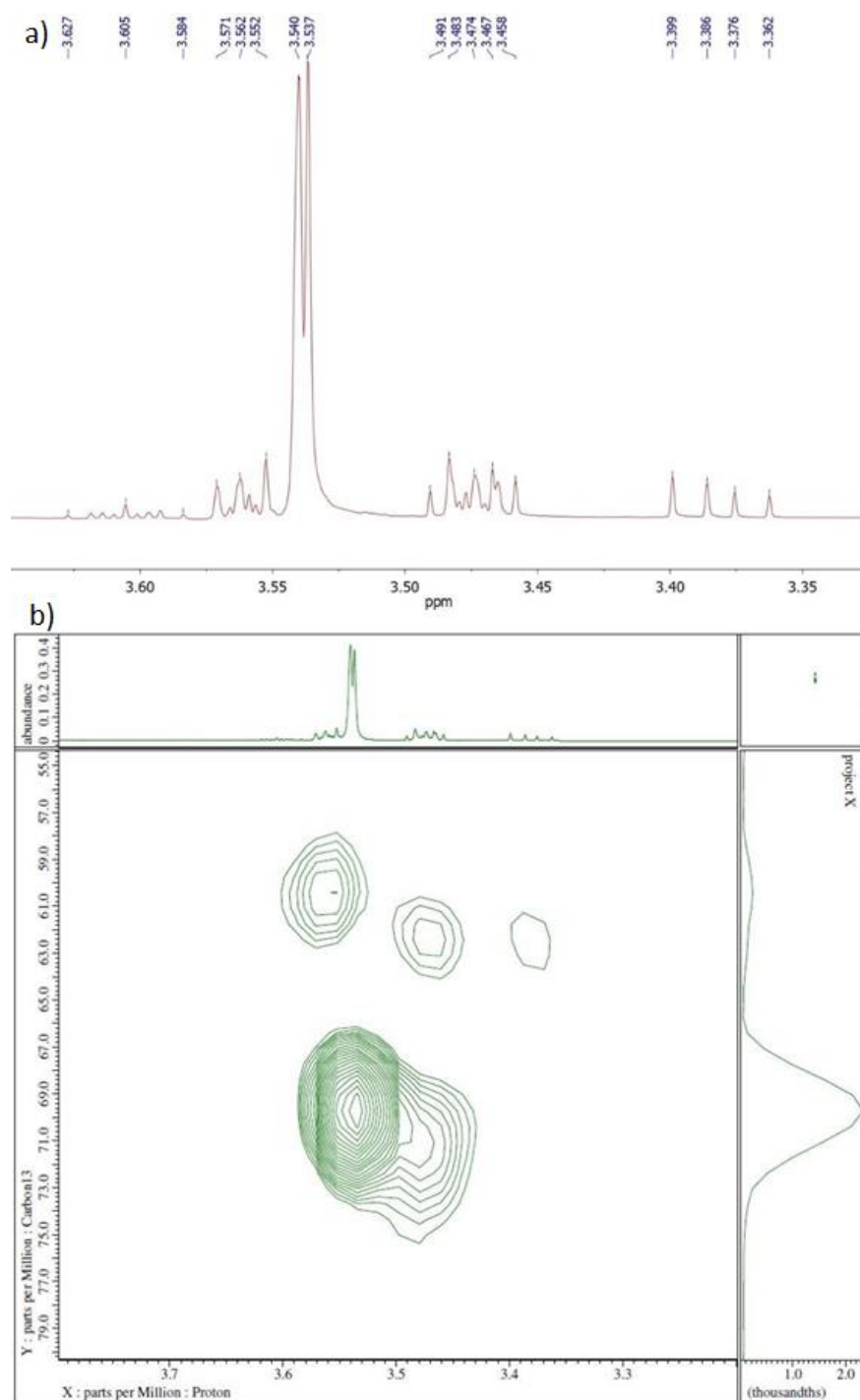


Figure 4.6: a)  $^1\text{H}$  and b) HSQC NMR spectra of ALBG.

Comparing the ALBG spectra with that of unmodified LBG (74), the most striking observation is the disappearance of the anomeric protons signals and a shift to a higher field of all the remaining signals. The disappearance of the anomeric proton can be explained by ring opening of 1,3-dioxane-type acetals of the polymer during the reduction phase of the reaction (197) which happens as represented in Figure 4.7.

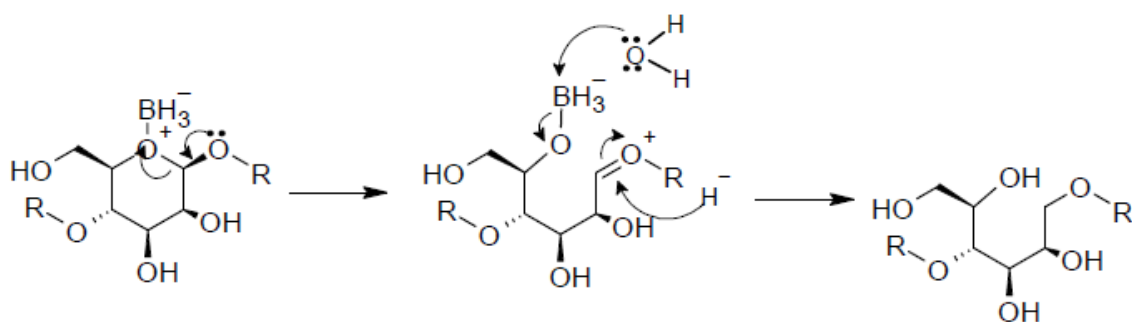


Figure 4.7: Regioselective ring opening of carbohydrates in a reductive medium.

Considering that not all mannose and galactose units reacted with periodate, various polymer fragments were obtained after degradation during the reduction phase (Figure 4.8), therefore explaining the complexity of the NMR spectra. Mannose and galactose units that were not cleaved by reaction with periodate produce fragments a) and b), respectively, while the fragments shown in c) and d) are a product of 1,3 cleavage mannose and e) and f) are products of the cleavage of oxidized galactose. It should be noted that fragment f) would be lost during dialysis due to its low size.

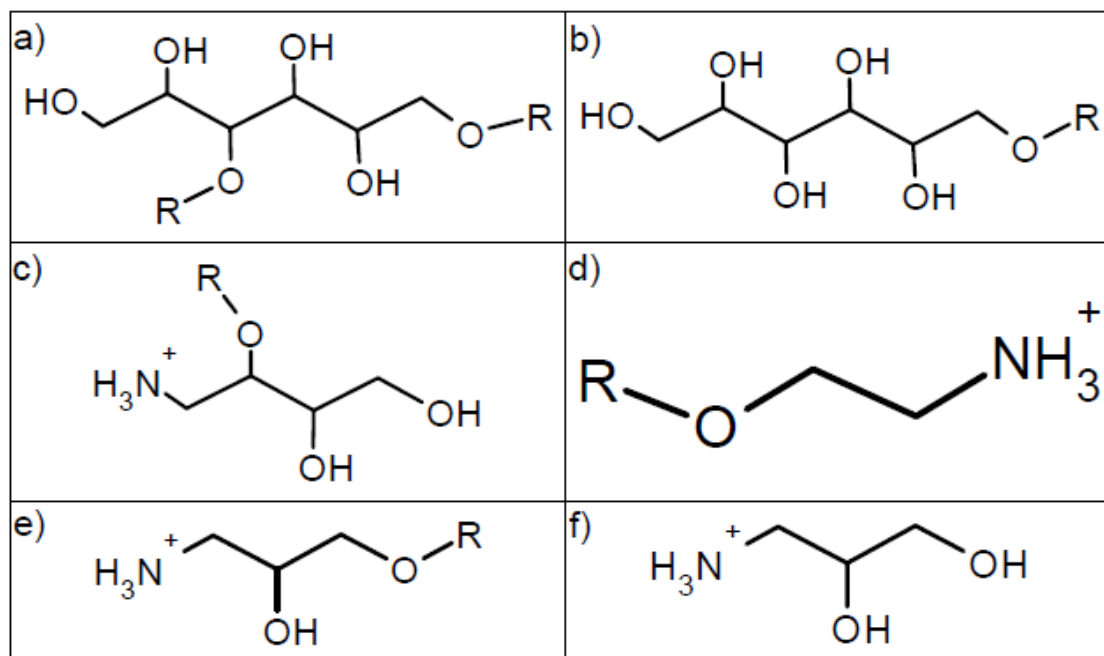


Figure 4.8: Fragments of ALBG after ring opening in reductive medium. a) and b) represent unoxidized mannose and galactose units after ring opening, c) and d) represent the fragments obtained after cleavage of oxidized mannose and e) and f) represent the fragments obtained after cleavage of oxidized galactose.

The dd at 3.380 ppm can be attributed to a proton of a CH<sub>2</sub> group next to a CHOH, since a geminal coupling (J=12 Hz) and a vicinal coupling (J=6.5 Hz) are observed. The signal centered at 3.474 can be attributed to protons of CH and CH<sub>2</sub>. The signal centered 3.539, is possibly a multiplet corresponding to protons of very similar CH that appears to be a dd due to low resolution of the NMR. The signal centered at 3.3562 can corresponds to protons of CH and CH<sub>2</sub>. The tt at 3.605 ppm can be attributed to the proton of a CH linked to the OH and two CH<sub>2</sub> (which exists in Figure 4.8, fragment e)).

## 4.2 ALBG/CRG nanoparticles

Considering a complete reaction, ALBG should present 4 charged groups per structural unit, with each structural unit weighting 956 g/mol (in chloride salt form). Therefore, the polymer in acidic aqueous solution has 0.00418 charges per gram. Comparing with the structure of CRG, constituted by structural units weighting 408 g/mol and bearing 1 charged groups, resulting in 0.00245 charges per gram, different charge ratios were estimated for the different mass ratios of polysaccharide, as shown in Table 4.1.

Table 4.1: Charge ratio of ALBG/CRG nanoparticles and concentration of each polysaccharide in the mixture.

Mass ratio ALBG/CRG	Charge ratio* (+/-)	[ALBG] (mg/mL)	[CRG] (mg/mL)
4/1	6.83	0.71	0.18
3/1	5.12	0.71	0.24
2/1	3.41	0.71	0.36
1/1	1.71	0.71	0.71
1/2	0.85	0.36	0.71
1/3	0.57	0.24	0.71
1/4	0.43	0.18	0.71

\*Theoretical charge ratio considering full conversion

PdI values range from 0 to 1, lower PdI indicating more uniform size distribution and stability. In the same manner, a smaller particle size and a higher zeta-potential also improve nanoparticle systems stability (198).

Results for the characterization of ALBG/CRG nanoparticles prepared with the LBG derivative obtained when using 2 equivalents of sodium periodate, did not show

effective formation of nanoparticles, which might indicate a lack of cationic groups in the derivative.

When 4 equivalents of sodium periodate were used, a larger amount of aldehyde groups were obtained and later turned into cationic ammonium groups. Using this derivative, the complexation with CRG allowed for the preparation of particles with adequate size, PdI and zeta-potential, as shown in Table 4.2. From the nanoparticles prepared, those corresponding to the 4/1, 1/3 and 1/4 mass ratios of ALBG to CRG displayed lower PdI, thus being the more adequate of the set for a possible application in drug delivery. As it can be seen in Figure 4.9, the particles size remains similar with the exception of those made with a 1/2 ratio. When the concentration of CRG is higher than that of ALBG, the particles display a negative zeta-potential. The particles produced generally present a larger size than that obtained in similar systems with other polysaccharides (31,145). Comparing to other LBG derivatives, the particles have similar characteristics (74). Still, the high standard deviation value for size should be noted. One possibility of optimization could be the addition of a crosslinking agent such as TPP (25). It should be noted that, after mixing the two polymer solutions, a precipitate could be observed for the 3/1, 2/1 and 1/1 mass ratios. This seems to imply that the charge ratio in these mixtures was near 1, making the repulsion between particles weak enough to form precipitate conglomerates. This fact may imply that only part of the amount of amine groups that should be present after the chemical reactions on LBG was, in fact, obtained.

Table 4.2: Physicochemical characteristics of ALBG/CRG nanoparticles (mean  $\pm$  SD; n = 3).

Mass ratio ALBG/CRG	Size (nm)	PdI	Zeta-potential (mV)
4/1	257.5 $\pm$ 139.2	0.30 $\pm$ 0.09	+9.0 $\pm$ 0.9
3/1	**	**	**
2/1	**	**	**
1/1	**	**	**
1/2	672.5 $\pm$ 326.7	0.59 $\pm$ 0.14	-38.3 $\pm$ 7.9
1/3	368.7 $\pm$ 95.1	0.42 $\pm$ 0.05	-43.6 $\pm$ 3.6
1/4	301.1 $\pm$ 62.5	0.44 $\pm$ 0.02	-40.3 $\pm$ 2.1

\*\*Precipitated.

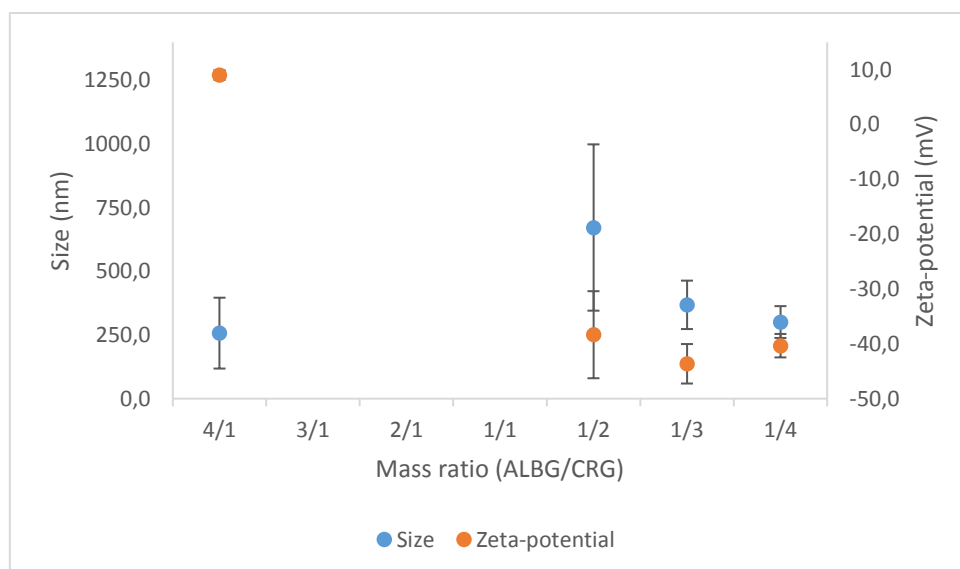


Figure 4.9: Effect of ALBG/CRG mass ratio on nanoparticle size and zeta potential (mean  $\pm$  SD,  $n = 3$ ).

Taking this hypothesis into account, the amount of sodium periodate was doubled to 8 equivalents to try to get the intended degree of substitution. Although doubling the amount of periodate did allow for more oxidation, the corresponding amination was not as effective. It has been observed (199) that polysaccharides oxidized with periodate depolymerized further, the higher the amount of periodate, and that is to be expected in these reactions.

As for ALBG obtained by reductive amination of C-6 oxidized LBG, reliable nanoparticles were not obtained upon combination with carrageenan. This is most probably due to lack of cationic groups on those LBG derivatives and lack of their uniform distribution along the polymer. Therefore, the chemical modifications should be attempted again with slight changes, namely more reagent equivalents and a better dissolution of LBG to provide a more uniform reaction.

## 5 Conclusions and future work

While the production of polysaccharide-based nanoparticles by polyelectrolyte complexation is common and useful for drug delivery purposes, options for cationic polysaccharides are lacking, with chitosan usually being the only one.

In this essay, it was attempted to synthesize cationic LBG derivatives through the addition of amine groups, which are positively charged in acid media. This addition was performed by oxidation of LBG alcohol groups to aldehyde, followed by reductive amination. Different reaction conditions and different oxidizing agents were tested (periodate, TEMPO, Oxone<sup>®</sup> and ammonium persulfate). The most successful reaction was performed using 4 equivalents of periodate, followed by reductive amination.

While the goal was to have 4 amine groups per structural unit, it seems that the degree of substitution was lower than expected. One of the main holdbacks of the reactions was the difficulty in getting a homogenous mixture. This possibly significantly reduced the degree of substitution of the polymer.

The yield of the reductive amination was also lower than expected, which is possibly due to cleavage in reductive medium. This hypothesis was confirmed by NMR analysis of ALBG, which supports the theory that there was degradation of the polymer.

The derivatives were used in nanoparticle production by polyelectrolyte complexation with CRG in different mass ratios. The mentioned flaws led to less than ideal nanoparticle production, with most derivatives not being able to create nanoparticles with CRG. The best particles (considering their size, zeta-potential and PDI) were obtained using ALBG produced through oxidation with 4 equivalents of periodate and CRG in mass ratios of 4/1, 1/3 or 1/4, which showed similar properties to other particles based on LBG derivatives, but with a higher deviation.

Taking all this into account, much more work needs to be put into producing cationic LBG derivatives. New strategies must be tried in order to get a more homogenous reaction mixture. These might include other purification procedures or the addition of salts in order to increase the solubility of the polymer. While the reaction employing periodate was the most successful in this project, the use of other reagents that oxidize the sixth carbon and maintain the main structure of the polymer should still be explored. The different reaction steps should also be optimized in terms of temperature and duration to get a higher yield and substitution degree. The polymer should also be further characterized by elemental analysis.

When it comes to the nanoparticles, different assays should also be performed, such as the determination of production yield and morphological analysis, in order to have

more understanding of the particles properties and possible applications. Finally, if possible, it should also be tested if these particles could be used as drug carriers.

## 6 References

1. Fathima N, Mamatha T, Qureshi HK, Anitha N, Rao JV. Drug-excipient interaction and its importance in dosage form development. *J Appl Pharm Sci.* 2011;1(6):66–71.
2. Zebroski B. *A Brief History of Pharmacy: Humanity's Search for Wellness.* Routledge; 2015.
3. Soleymani S, Zargarani A. A Historical Report on Preparing Sustained Release Dosage Forms for Addicts in Medieval Persia, 16th Century AD. *Subst Use Misuse.* 2018;53(10):1726–9.
4. Lee PI, Li J-X. Evolution of Oral Controlled Release Dosage Forms. In: Wen H, Park K, editors. *Oral Controlled Release Formulation Design and Drug Delivery.* John Wiley & Sons; 2010. p. 21–31.
5. Yun YH, Lee BK, Park K. Controlled Drug Delivery: Historical perspective for the next generation. *J Control Release.* 2015;219:2–7.
6. Sung Wan Kim, Chaul Min Pahi, Kimiko M, Seminoff LA, Holmberg DL, Gleeson JM, et al. Self-regulated glycosylated insulin delivery. *J Control Release.* 1990;11(1–3):193–201.
7. Klumb LA, Horbett TA. Design of insulin delivery devices based on glucose sensitive membranes. *J Control Release.* 1992;18(1):59–80.
8. Wolinsky JB, Colson YL, Grinstaff MW. Local drug delivery strategies for cancer treatment: Gels, nanoparticles, polymeric films, rods, and wafers. *J Control Release.* 2012;159(1):14–26.
9. MG K, Krenn V, F H. History and Possible Uses of Nanomedicine Based on Nanoparticles and Nanotechnological Progress. *J Nanomed Nanotechnol.* 2015;6(6).
10. FDA. Guidance for industry considering whether an FDA-regulated product involves the application of nanotechnology. 2014;
11. Ensign LM, Cone R, Hanes J. Oral drug delivery with polymeric nanoparticles: The gastrointestinal mucus barriers. *Adv Drug Deliv Rev.* 2012;64(6):557–70.
12. Huo M, Chen Y, Shi J. Triggered-release drug delivery nanosystems for cancer therapy by intravenous injection: where are we now? *Expert Opin Drug Deliv.* 2016;13(9):1195–8.
13. Goyal R, Macri LK, Kaplan HM, Kohn J. Nanoparticles and nanofibers for topical drug delivery. *J Control Release.* 2016;240:77–92.
14. Pontes JF, Grenha A. Multifunctional nanocarriers for lung drug delivery. *Nanomaterials.* 2020;10(2):183.
15. Riley MK, Vermerris W. Recent advances in nanomaterials for gene delivery—A review. *Nanomaterials.* 2017;7(5):94.
16. Bitoque DB, Rosa da Costa AM, Silva GA. Insights on the intracellular trafficking of PDMAEMA gene therapy vectors. *Mater Sci Eng C.* 2018;93:277–88.

17. Yu M, Wu J, Shi J, Farokhzad OC. Nanotechnology for protein delivery: Overview and perspectives. *J Control Release*. 2015/10/13. 2016;240:24–37.
18. Cho EJ, Holback H, Liu KC, Abouelmagd SA, Park J, Yeo Y. Nanoparticle Characterization: State of the Art, Challenges, and Emerging Technologies. *Mol Pharm*. 2013;10(6):2093–110.
19. Anu Mary Ealia S, Saravanakumar MP. A review on the classification, characterisation, synthesis of nanoparticles and their application. *IOP Conf Ser Mater Sci Eng*. 2017;263:32019.
20. Son G-H, Lee B-J, Cho C-W. Mechanisms of drug release from advanced drug formulations such as polymeric-based drug-delivery systems and lipid nanoparticles. *J Pharm Investig*. 2017;47(4):287–96.
21. Lima AC, Sher P, Mano JF. Production methodologies of polymeric and hydrogel particles for drug delivery applications. *Expert Opin Drug Deliv*. 2012;9(2):231–48.
22. Grenha A. Chitosan nanoparticles : a survey of preparation methods. *J Drug Target*. 2012;20(4):291–300.
23. Nait Mohamed FA, Laraba-Djebari F. Development and characterization of a new carrier for vaccine delivery based on calcium-alginate nanoparticles: Safe immunoprotective approach against scorpion envenoming. *Vaccine*. 2016;34(24):2692–9.
24. Fan W, Yan W, Xu Z, Ni H. Formation mechanism of monodisperse, low molecular weight chitosan nanoparticles by ionic gelation technique. *Colloids Surfaces B Biointerfaces*. 2012;90:21–7.
25. Rodrigues S, Rosa AM, Grenha A. Chitosan / carrageenan nanoparticles : Effect of cross-linking with tripolyphosphate and charge ratios. *Carbohydr Polym*. 2012;89(1):282–9.
26. Ciro Y, Rojas J, Oñate-Garzon J, Salamanca CH. Synthesis, Characterisation and Biological Evaluation of Ampicillin–Chitosan–Polyanion Nanoparticles Produced by Ionic Gelation and Polyelectrolyte Complexation Assisted by High-Intensity Sonication. Vol. 11, *Polymers* . 2019.
27. Sarmiento B, Ferreira D, Veiga F, Ribeiro A. Characterization of insulin-loaded alginate nanoparticles produced by ionotropic pre-gelation through DSC and FTIR studies. *Carbohydr Polym*. 2006;66(1):1–7.
28. Meka VS, Sing MKG, Pichika MR, Nali SR, Kolapalli VRM, Kesharwani P. A comprehensive review on polyelectrolyte complexes. *Drug Discov Today*. 2017;22(11):1697–706.
29. Grenha A, Gomes ME, Rodrigues M, Santo VE, Mano JF, Neves NM, et al. Development of new chitosan/carrageenan nanoparticles for drug delivery applications. *J Biomed Mater Res - Part A*. 2010;92(4):1265–72.
30. Braz L, Grenha A, Ferreira D, Rosa AM, Gamazo C, Sarmiento B. Chitosan / sulfated locust bean gum nanoparticles : In vitro and in vivo evaluation towards an application in oral immunization. *Int J Biol Macromol*. 2017;96:786–97.

31. Dionísio M, Cordeiro C, Remuñán-lópez C, Seijo B, Rosa AM, Grenha A. Pullulan-based nanoparticles as carriers for transmucosal protein delivery. *Eur J Pharm Sci.* 2013;50(1):102–13.
32. Cunha L, Rodrigues S, Rosa da Costa MA, Faleiro LM, Buttini F, Grenha A. Inhalable Fucoïdan Microparticles Combining Two Antitubercular Drugs with Potential Application in Pulmonary Tuberculosis Therapy. Vol. 10, *Polymers.* 2018. p. 636.
33. Sook M, Eun H, Lee J, Koo H, Lee S, Hwa S, et al. Polysaccharide-based Nanoparticles for Gene Delivery. *Top Curr Chem.* 2017;375(2):65–83.
34. Yu Y, Shen M, Song Q, Xie J. Biological activities and pharmaceutical applications of polysaccharide from natural resources: A review. *Carbohydr Polym.* 2018;183:91–101.
35. Malafaya PB, Silva GA, Reis RL. Natural–origin polymers as carriers and scaffolds for biomolecules and cell delivery in tissue engineering applications. *Adv Drug Deliv Rev.* 2007;59(4–5):207–33.
36. Kajiwara K, Miyamoto T. Polysaccharides: structural diversity and functional versatility. In: Dumitriu S, editor. *Polysaccharides: structural diversity and functional versatility.* CRC press; 2004. p. 19–41.
37. Shi L. Bioactivities, isolation and purification methods of polysaccharides from natural products: A review. *Int J Biol Macromol.* 2016;92:37–48.
38. Shariatnia Z. Pharmaceutical applications of natural polysaccharides. In: Hasnain MS, Nayak AK, editors. *Natural Polysaccharides in Drug Delivery and Biomedical Applications.* Academic Press; 2019. p. 15–50.
39. Smidsrød O, Skjåk-Bræk G. Alginate as immobilization matrix for cells. *Trends Biotechnol.* 1990;8:71–8.
40. Lee KY, Mooney DJ. Alginate: Properties and biomedical applications. *Prog Polym Sci.* 2012;37(1):106–26.
41. Paques JP, Van Der Linden E, Van Rijn CJM, Sagis LMC. Preparation methods of alginate nanoparticles. *Adv Colloid Interface Sci.* 2014;209:163–71.
42. Sun J, Tan H. Alginate-based biomaterials for regenerative medicine applications. *Materials (Basel).* 2013;6(4):1285–309.
43. Jia J, Richards DJ, Pollard S, Tan Y, Rodriguez J, Visconti RP, et al. Engineering alginate as bioink for bioprinting. *Acta Biomater.* 2014;10(10):4323–31.
44. Yang JS, Xie YJ, He W. Research progress on chemical modification of alginate: A review. *Carbohydr Polym.* 2011;84(1):33–9.
45. Necas J, Bartosikova L. Carrageenan: a review. *Vet Med (Praha).* 2013;58(4):187–205.
46. Wijesekara I, Pangestuti R, Kim SK. Biological activities and potential health benefits of sulfated polysaccharides derived from marine algae. *Carbohydr Polym.* 2011;84(1):14–21.
47. Chen HM, Yan XJ, Wang F, Xu WF, Zhang L. Assessment of the oxidative cellular

- toxicity of a  $\kappa$ -carrageenan oxidative degradation product towards Caco-2 cells. *Food Res Int.* 2010;43(10):2390–401.
48. Li L, Wang L, Shao Y, Tian YE, Li C, Li Y, et al. Elucidation of Release Characteristics of Highly Soluble Drug Trimetazidine Hydrochloride from Chitosan-Carrageenan Matrix Tablets. *J Pharm Sci.* 2013;102(8):2644–54.
  49. Miyazaki S, Ishitani M, Takahashi A, Shimoyama T, Itoh K, Attwood D. Carrageenan Gels for Oral Sustained Delivery of Acetaminophen to Dysphagic Patients. *Biol Pharm Bull.* 2011;34(1):164–6.
  50. Mao S, Guo C, Shi Y, Li LC. Recent advances in polymeric microspheres for parenteral drug delivery—part 2. *Expert Opin Drug Deliv.* 2012;9(10):1209–23.
  51. Grenha A, Gomes ME, Rodrigues M, Santo VE, Mano JF, Neves NM, et al. Development of new chitosan/carrageenan nanoparticles for drug delivery applications. *J Biomed Mater Res Part A.* 2010;92(4):1265–72.
  52. Li L, Ni R, Shao Y, Mao S. Carrageenan and its applications in drug delivery. *Carbohydr Polym.* 2014;103:1–11.
  53. Kim C-J. *Advanced pharmaceuticals: Physicochemical principles.* CRC Press LLC. 2004. 417–499 p.
  54. Klemm D, Heublein B, Fink H-P, Bohn A. Cellulose: Fascinating Biopolymer and Sustainable Raw Material. *Angew Chemie Int Ed.* 2005;44(22):3358–93.
  55. Ishikawa A, Okano T, Sugiyama J. Fine structure and tensile properties of ramie fibres in the crystalline form of cellulose I, II, III and IVI. *Polymer (Guildf).* 1997;38(2):463–8.
  56. Huber T, Müssig J, Curnow O, Pang S, Bickerton S, Staiger MP. A critical review of all-cellulose composites. *J Mater Sci.* 2012;47(3):1171–86.
  57. Lu P, Hsieh Y-L. Preparation and properties of cellulose nanocrystals: Rods, spheres, and network. *Carbohydr Polym.* 2010;82(2):329–36.
  58. Yu H, Qin Z, Liang B, Liu N, Zhou Z, Chen L. Facile extraction of thermally stable cellulose nanocrystals with a high yield of 93% through hydrochloric acid hydrolysis under hydrothermal conditions. *J Mater Chem A.* 2013;1(12):3938–44.
  59. Kontturi E, Meriluoto A, Penttilä PA, Baccile N, Malho J-M, Potthast A, et al. Degradation and Crystallization of Cellulose in Hydrogen Chloride Vapor for High-Yield Isolation of Cellulose Nanocrystals. *Angew Chemie Int Ed.* 2016;55(46):14455–8.
  60. Abdul Khalil HPS, Davoudpour Y, Islam MN, Mustapha A, Sudesh K, Dungani R, et al. Production and modification of nanofibrillated cellulose using various mechanical processes: A review. *Carbohydr Polym.* 2014;99:649–65.
  61. Jonoobi M, Oladi R, Davoudpour Y, Oksman K, Dufresne A, Hamzeh Y, et al. Different preparation methods and properties of nanostructured cellulose from various natural resources and residues: a review. *Cellulose.* 2015;22(2):935–69.
  62. Yu H-Y, Wang C, Abdalkarim SYH. Cellulose nanocrystals/polyethylene glycol as bifunctional reinforcing/compatibilizing agents in poly(lactic acid) nanofibers for controlling long-term in vitro drug release. *Cellulose.* 2017;24(10):4461–77.

63. Cheng M, Qin Z, Hu S, Dong S, Ren Z, Yu H. Achieving Long-Term Sustained Drug Delivery for Electrospun Biopolyester Nanofibrous Membranes by Introducing Cellulose Nanocrystals. *ACS Biomater Sci Eng.* 2017;3(8):1666–76.
64. He X, Xiao Q, Lu C, Wang Y, Zhang X, Zhao J, et al. Uniaxially Aligned Electrospun All-Cellulose Nanocomposite Nanofibers Reinforced with Cellulose Nanocrystals: Scaffold for Tissue Engineering. *Biomacromolecules.* 2014;15(2):618–27.
65. Abdel-Rahman RM, Hrdina R, Abdel-Mohsen AM, Fouda MMG, Soliman AY, Mohamed FK, et al. Chitin and chitosan from Brazilian Atlantic Coast: Isolation, characterization and antibacterial activity. *Int J Biol Macromol.* 2015;80:107–20.
66. Younes I, Rinaudo M. Chitin and chitosan preparation from marine sources. Structure, properties and applications. *Mar Drugs.* 2015;13(3):1133–74.
67. Sudarshan NR, Hoover DG, Knorr D. Antibacterial action of chitosan. *Food Biotechnol.* 1992;6(3):257–72.
68. Kean T, Thanou M. Biodegradation, biodistribution and toxicity of chitosan. *Adv Drug Deliv Rev.* 2010;62(1):3–11.
69. Hejjaji EMA, Smith AM, Morris GA. Evaluation of the mucoadhesive properties of chitosan nanoparticles prepared using different chitosan to tripolyphosphate (CS:TPP) ratios. *Int J Biol Macromol.* 2018;120:1610–7.
70. Cheung CR, Ng BT, Wong HJ, Chan YW. Chitosan: An Update on Potential Biomedical and Pharmaceutical Applications. Vol. 13, *Marine Drugs.* 2015. p. 5156–86.
71. Martínez-Camacho AP, Cortez-Rocha MO, Ezquerro-Brauer JM, Graciano-Verdugo AZ, Rodriguez-Félix F, Castillo-Ortega MM, et al. Chitosan composite films: Thermal, structural, mechanical and antifungal properties. *Carbohydr Polym.* 2010;82(2):305–15.
72. Yen M-T, Yang J-H, Mau J-L. Antioxidant properties of chitosan from crab shells. *Carbohydr Polym.* 2008;74(4):840–4.
73. Azuma K, Osaki T, Minami S, Okamoto Y. Anticancer and Anti-Inflammatory Properties of Chitin and Chitosan Oligosaccharides. Vol. 6, *Journal of Functional Biomaterials.* 2015. p. 33–49.
74. Braz L, Grenha A, Corvo MC, Paulo J, Ferreira D, Sarmiento B, et al. Synthesis and characterization of Locust Bean Gum derivatives and their application in the production of nanoparticles. *Carbohydr Polym.* 2018;181:974–85.
75. Luo Y, Wang Q. Recent development of chitosan-based polyelectrolyte complexes with natural polysaccharides for drug delivery. *Int J Biol Macromol.* 2014;64:353–67.
76. Cunha L, Rodrigues S, Rosa da Costa AM, Faleiro L, Buttini F, Grenha A. Inhalable chitosan microparticles for simultaneous delivery of isoniazid and rifabutin in lung tuberculosis treatment. *Drug Dev Ind Pharm.* 2019;45(8):1313–20.
77. Saito H, Misaki A, Harada T. A Comparison of the Structure of Curdlan and

- Pachyman. *Agric Biol Chem*. 1968;32(10):1261–9.
78. Futatsuyama H, Yui T, Ogawa K. Viscometry of Curdlan, a Linear (1→3)- $\beta$ -D-Glucan, in DMSO or Alkaline Solutions. *Biosci Biotechnol Biochem*. 1999;63(8):1481–3.
  79. Zhang R, Edgar KJ. Properties, chemistry, and applications of the bioactive polysaccharide curdlan. *Biomacromolecules*. 2014;15(4):1079–96.
  80. Maeda I, Saito H, Masada M, Misaki A, Harada T. Properties of Gels Formed by Heat Treatment of Curdlan, a Bacterial  $\beta$ -1,3 Glucan. *Agric Biol Chem*. 1967;31(10):1184–8.
  81. Tang J, Zhen H, Wang N, Yan Q, Jing H, Jiang Z. Curdlan oligosaccharides having higher immunostimulatory activity than curdlan in mice treated with cyclophosphamide. *Carbohydr Polym*. 2019;207:131–42.
  82. Rui K, Tian J, Tang X, Ma J, Xu P, Tian X, et al. Curdlan blocks the immune suppression by myeloid-derived suppressor cells and reduces tumor burden. *Immunol Res*. 2016;64(4):931–9.
  83. Yan JK, Ma H Le, Chen X, Pei JJ, Wang Z Bin, Wu JY. Self-aggregated nanoparticles of carboxylic curdlan-deoxycholic acid conjugates as a carrier of doxorubicin. *Int J Biol Macromol*. 2015;72:333–40.
  84. Li L, Gao F, Tang H, Bai Y, Li R, Li X, et al. Self-assembled nanoparticles of cholesterol-conjugated carboxymethyl curdlan as a novel carrier of epirubicin. *Nanotechnology*. 2010;21:265601.
  85. Popescu I, Pelin IM, Butnaru M, Fundueanu G, Suflet DM. Phosphorylated curdlan microgels. Preparation, characterization, and in vitro drug release studies. *Carbohydr Polym*. 2013;94(2):889–98.
  86. Cai Z, Zhang H. Recent progress on curdlan provided by functionalization strategies. *Food Hydrocoll*. 2017;68:128–35.
  87. Neely WB. Dextran: Structure and Synthesis. Wolfrom ML, Tipson RSBT-A in CC, editors. *Adv Carbohydr Chem*. 1961;15:341–69.
  88. Santos M, Rodrigues A, Teixeira JA. Production of dextran and fructose from carob pod extract and cheese whey by *Leuconostoc mesenteroides* NRRL B512(f). *Biochem Eng J*. 2005;25(1):1–6.
  89. Barker PE, Ajongwen NJ. The production of the enzyme dextransucrase using nonaerated fermentation techniques. *Biotechnol Bioeng*. 1991;37(8):703–7.
  90. TSUCHIYA HM, KOEPSSELL HJ, CORMAN J, BRYANT G, BOGARD MO, FEGER VH, et al. The effect of certain cultural factors on production of dextransucrase by *Leuconostoc mesenteroides*. *J Bacteriol*. 1952;64(4):521–6.
  91. Jeanes A, Haynes WC, Wilham CA, Rankin JC, Melvin EH, Austin MJ, et al. Characterization and Classification of Dextran from Ninety-six Strains of Bacteria1b. *J Am Chem Soc*. 1954;76(20):5041–52.
  92. Van Tomme SR, Hennink WE. Biodegradable dextran hydrogels for protein delivery applications. *Expert Rev Med Devices*. 2007;4(2):147–64.

93. Khalikova E, Susi P, Korpela T. Microbial dextran-hydrolyzing enzymes: fundamentals and applications. *Microbiol Mol Biol Rev.* 2005;69(2):306–25.
94. Mehvar R. Dextran for targeted and sustained delivery of therapeutic and imaging agents. *J Control Release.* 2000;69(1):1–25.
95. Maia J, Evangelista MB, Gil H, Ferreira L. Dextran-based materials for biomedical applications. *Res Signpost.* 2014;37661:31–53.
96. Banerjee A, Bandopadhyay R. Use of dextran nanoparticle: A paradigm shift in bacterial exopolysaccharide based biomedical applications. *Int J Biol Macromol.* 2016;87:295–301.
97. Du Y-Z, Weng Q, Yuan H, Hu F-Q. Synthesis and Antitumor Activity of Stearate-g-dextran Micelles for Intracellular Doxorubicin Delivery. *ACS Nano.* 2010;4(11):6894–902.
98. Sun G, Zhang X, Shen Y-I, Sebastian R, Dickinson LE, Fox-Talbot K, et al. Dextran hydrogel scaffolds enhance angiogenic responses and promote complete skin regeneration during burn wound healing. *Proc Natl Acad Sci.* 2011;108(52):20976 LP – 20981.
99. Li M, Tang Z, Zhang Y, Lv S, Li Q, Chen X. Targeted delivery of cisplatin by LHRH-peptide conjugated dextran nanoparticles suppresses breast cancer growth and metastasis. *Acta Biomater.* 2015;18:132–43.
100. Valente JFA, Gaspar VM, Antunes BP, Countinho P, Correia IJ. Microencapsulated chitosan–dextran sulfate nanoparticles for controlled delivery of bioactive molecules and cells in bone regeneration. *Polymer (Guildf).* 2013;54(1):5–15.
101. Nishino T, Nishioka C, Ura H, Nagumo T. Isolation and partial characterization of a novel amino sugar-containing fucan sulfate from commercial *Fucus vesiculosus* fucoidan t. *Carbohydr Res.* 1994;255:213–24.
102. Chizhov AO, Dell A, Morris HR, Haslam SM, McDowell RA, Shashkov AS, et al. A study of fucoidan from the brown seaweed *Chorda filum*. *Carbohydr Res.* 1999;320(1):108–19.
103. Bilan MI, Grachev AA, Ustuzhanina NE, Shashkov AS, Nifantiev NE, Usov AI. Structure of a fucoidan from the brown seaweed *Fucus evanescens* C.Ag. *Carbohydr Res.* 2002;337(8):719–30.
104. Li B, Lu F, Wei X, Zhao R. Fucoidan: Structure and Bioactivity. *Molecules.* 2008;13(8):1671–95.
105. Cumashi A, Ushakova NA, Preobrazhenskaya ME, D’Incecco A, Piccoli A, Totani L, et al. A comparative study of the anti-inflammatory, anticoagulant, antiangiogenic, and antiadhesive activities of nine different fucoidans from brown seaweeds. *Glycobiology.* 2007;17(5):541–52.
106. Fan L, Tongchun T, Yanchun S, Yang L, Shaolun Z. Study on anti-virus effect of fucoidan in vitro [Internet]. Vol. 21, Baiqiuen Yike Daxue Xuebao. School of Basic Medical Sciences, Norman Bethune University of Medical Sciences. Changchun 130021, Jilin; China; 1995. p. 255–7.

107. Ponce NMA, Pujol CA, Damonte EB, Flores ML, Stortz CA. Fucoidans from the brown seaweed *Adenocystis utricularis*: extraction methods, antiviral activity and structural studies. *Carbohydr Res.* 2003;338(2):153–65.
108. Mak W, Hamid N, Liu T, Lu J, White WL. Fucoidan from New Zealand *Undaria pinnatifida*: Monthly variations and determination of antioxidant activities. *Carbohydr Polym.* 2013;95(1):606–14.
109. Yoo HJ, You D-J, Lee K-W. Characterization and Immunomodulatory Effects of High Molecular Weight Fucoidan Fraction from the Sporophyll of *Undaria pinnatifida* in Cyclophosphamide-Induced Immunosuppressed Mice. *Mar Drugs.* 2019;17(8):447.
110. Park HY, Han MH, Park C, Jin C-Y, Kim G-Y, Choi I-W, et al. Anti-inflammatory effects of fucoidan through inhibition of NF- $\kappa$ B, MAPK and Akt activation in lipopolysaccharide-induced BV2 microglia cells. *Food Chem Toxicol.* 2011;49(8):1745–52.
111. Hayashi S, Itoh A, Isoda K, Kondoh M, Kawase M, Yagi K. Fucoidan partly prevents CCl<sub>4</sub>-induced liver fibrosis. *Eur J Pharmacol.* 2008;580(3):380–4.
112. Wang Y, Su W, Zhang C, Xue C, Chang Y, Wu X, et al. Protective effect of sea cucumber (*Acaudina molpadioides*) fucoidan against ethanol-induced gastric damage. *Food Chem.* 2012;133(4):1414–9.
113. Wang J, Zhang Q, Jin W, Niu X, Zhang H. Effects and mechanism of low molecular weight fucoidan in mitigating the peroxidative and renal damage induced by adenine. *Carbohydr Polym.* 2011;84(1):417–23.
114. Huang L, Wen K, Gao X, Liu Y. Hypolipidemic effect of fucoidan from *Laminaria japonica* in hyperlipidemic rats. *Pharm Biol.* 2010;48(4):422–6.
115. Fernando IPS, Kim D, Nah J, Jeon Y. Advances in functionalizing fucoidans and alginates ( bio ) polymers by structural modifications : A review. *Chem Eng J.* 2019;355:33–48.
116. Oliveira C, Neves NM, Reis RL, Martins A, Silva TH. A review on fucoidan antitumor strategies: From a biological active agent to a structural component of fucoidan-based systems. *Carbohydr Polym.* 2020;239:116131.
117. Cunha L, Rosa da Costa AM, Lourenço JP, Buttini F, Grenha A. Spray-dried fucoidan microparticles for pulmonary delivery of antitubercular drugs. *J Microencapsul.* 2018;35(4):392–405.
118. Weissmann B, Meyer K. The Structure of Hyalobiuronic Acid and of Hyaluronic Acid from Umbilical Cord<sup>1,2</sup>. *J Am Chem Soc.* 1954;76(7):1753–7.
119. Chong BF, Blank LM, McLaughlin R, Nielsen LK. Microbial hyaluronic acid production. *Appl Microbiol Biotechnol.* 2005;66(4):341–51.
120. O'Regan M, Martini I, Crescenzi F, De Luca C, Lansing M. Molecular mechanisms and genetics of hyaluronan biosynthesis. *Int J Biol Macromol.* 1994;16(6):283–6.
121. Moreland LW. Intra-articular hyaluronan (hyaluronic acid) and hylans for the treatment of osteoarthritis: mechanisms of action. *Arthritis Res Ther.* 2003;5(2):54.

122. Barbucci R, Lamponi S, Borzacchiello A, Ambrosio L, Fini M, Torricelli P, et al. Hyaluronic acid hydrogel in the treatment of osteoarthritis. *Biomaterials*. 2002;23(23):4503–13.
123. Salwowska NM, Bebenek KA, Żądło DA, Wcisło-Dziadecka DL. Physicochemical properties and application of hyaluronic acid: a systematic review. *J Cosmet Dermatol*. 2016;15(4):520–6.
124. Widjaja LK, Bora M, Chan PNP, Lipik V, Wong TTL, Venkatraman SS. Hyaluronic acid-based nanocomposite hydrogels for ocular drug delivery applications. *J Biomed Mater Res Part A*. 2014;102(9):3056–65.
125. Fallacara A. Hyaluronic Acid in the Third Millennium. *Polymers (Basel)*. 2018;10(7):701.
126. Yu M, Jambhrunkar S, Thorn P, Chen J, Gu W, Yu C. Hyaluronic acid modified mesoporous silica nanoparticles for targeted drug delivery to CD44-overexpressing cancer cells. *Nanoscale*. 2013;5(1):178–83.
127. Lee D-E, Kim AY, Yoon HY, Choi KY, Kwon IC, Jeong SY, et al. Amphiphilic hyaluronic acid-based nanoparticles for tumor-specific optical/MR dual imaging. *J Mater Chem*. 2012;22(21):10444–7.
128. Hirakura T, Yasugi K, Nemoto T, Sato M, Shimoboji T, Aso Y, et al. Hybrid hyaluronan hydrogel encapsulating nanogel as a protein nanocarrier: New system for sustained delivery of protein with a chaperone-like function. *J Control Release*. 2010;142(3):483–9.
129. Yao J, Fan Y, Du R, Zhou J, Lu Y, Wang W, et al. Amphoteric hyaluronic acid derivative for targeting gene delivery. *Biomaterials*. 2010;31(35):9357–65.
130. Huang G, Huang H. Application of hyaluronic acid as carriers in drug delivery. *Drug Deliv*. 2018;25(1):766–72.
131. Kawamura Y, Ph D, Smith J, Ph D. 82nd JECFA - Chemical and Technical Assessment (CTA), 2016 © FAO 2016 Carob Bean Gum Chemical and Technical Assessment (CTA). 2016;
132. Barak S, Mudgil D. Locust bean gum: Processing, properties and food applications-A review. *Int J Biol Macromol*. 2014;66:74–80.
133. Dionísio M, Grenha A. Locust bean gum: Exploring its potential for biopharmaceutical applications. *J Pharm Bioallied Sci*. 2012;4(3):175–85.
134. Kaity S, Isaac J, Ghosh A. Interpenetrating polymer network of locust bean gum-poly (vinyl alcohol) for controlled release drug delivery. *Carbohydr Polym*. 2013;94(1):456–67.
135. Martins JT, Cerqueira MA, Bourbon AI, Pinheiro AC, Souza BWS, Vicente AA. Synergistic effects between  $\kappa$ -carrageenan and locust bean gum on physicochemical properties of edible films made thereof. *Food Hydrocoll*. 2012;29(2):280–9.
136. Leathers TD. Biotechnological production and applications of pullulan. *Appl Microbiol Biotechnol*. 2003;62(5):468–73.
137. Bender H, Lehmann J, Wallenfels K. Pullulan, ein extracelluläres Glucan von

- Pullularia pullulans. *Biochim Biophys Acta*. 1959;36(2):309–16.
138. Kimoto T, Shibuya T, Shiobara S. Safety studies of a novel starch, pullulan: Chronic toxicity in rats and bacterial mutagenicity. *Food Chem Toxicol*. 1997;35(3–4):323–9.
  139. Shingel KI. Current knowledge on biosynthesis, biological activity, and chemical modification of the exopolysaccharide, pullulan. *Carbohydr Res*. 2004;339(3):447–60.
  140. Zhang H, Li X, Gao F, Liu L, Zhou Z, Zhang Q. Preparation of folate-modified pullulan acetate nanoparticles for tumor-targeted drug delivery. *Drug Deliv*. 2010;17(1):48–57.
  141. Singh RS, Kaur N, Kennedy JF. Pullulan and pullulan derivatives as promising biomolecules for drug and gene targeting. *Carbohydr Polym*. 2015;123:190–207.
  142. Prajapati VD, Jani GK, Khanda SM. Pullulan: An exopolysaccharide and its various applications. *Carbohydr Polym*. 2013;95(1):540–9.
  143. Huang L, Wang Y, Ling X, Chaurasiya B, Yang C, Du Y, et al. Efficient delivery of paclitaxel into ASGPR over-expressed cancer cells using reversibly stabilized multifunctional pullulan nanoparticles. *Carbohydr Polym*. 2017;159:178–87.
  144. Grigoras AG. Drug delivery systems using pullulan, a biocompatible polysaccharide produced by fungal fermentation of starch. *Environ Chem Lett*. 2019;17(3):1209–23.
  145. Dionísio M, Braz L, Corvo M, Lourenc JP, Costa AMR. Charged pullulan derivatives for the development of nanocarriers by polyelectrolyte complexation. *Int J Biol Macromol*. 2016;86:129–38.
  146. Ellis RP, Cochrane MP, Dale MFB, Duffus CM, Lynn A, Morrison IM, et al. Starch production and industrial use. *J Sci Food Agric*. 1998;77(3):289–311.
  147. Builders PF, Arhewoh MI. Pharmaceutical applications of native starch in conventional drug delivery. *Starch - Stärke*. 2016;68(9–10):864–73.
  148. Masina N, Choonara YE, Kumar P, du Toit LC, Govender M, Indermun S, et al. A review of the chemical modification techniques of starch. *Carbohydr Polym*. 2017;157:1226–36.
  149. Rodrigues A, Emeje M. Recent applications of starch derivatives in nanodrug delivery. *Carbohydr Polym*. 2012;87(2):987–94.
  150. Kim SK, Park H, Lee JM, Na K, Lee ES. pH-responsive starch microparticles for a tumor-targeting implant. *Polym Adv Technol*. 2018;29:1372–6.
  151. Putro JN, Ismadji S, Gunarto C, Soetaredjo FE, Ju YH. A study of anionic, cationic, and nonionic surfactants modified starch nanoparticles for hydrophobic drug loading and release. *J Mol Liq*. 2020;298:112034.
  152. Yang J, Li F, Li M, Zhang S, Liu J, Liang C, et al. Fabrication and characterization of hollow starch nanoparticles by gelation process for drug delivery application. *Carbohydr Polym*. 2017;173:223–32.
  153. Li S, Xiong Q, Lai X, Li X, Wan M, Zhang J, et al. Molecular Modification of

- Polysaccharides and Resulting Bioactivities. *Compr Rev Food Sci Food Saf.* 2016;15(2):237–50.
154. Xu Y, Wu Y, Sun P, Zhang F, Linhardt RJ, Zhang A. Chemically modified polysaccharides : Synthesis , characterization , structure activity relationships of action. *Int J Biol Macromol.* 2019;132:970–7.
  155. Liu J, Willfo S, Xu C. A review of bioactive plant polysaccharides : Biological activities , functionalization , and biomedical applications. *Bioact Carbohydrates Diet Fibre.* 2015;5(1):31–61.
  156. Bobbiw BYJM. Periodate Oxidation of Carbohydrates. *Adv Carbohydr Chem.* 1956;11:1–41.
  157. Yuan X, Li H, Zhu X, Woo H. Self-aggregated nanoparticles composed of periodate-oxidized dextran and cholic acid : preparation , stabilization and in-vitro drug release. *J Chem Technol Biotechnol.* 2006;81(5):746–54.
  158. Zhang D, Chen L, Zang C, Chen Y, Lin H. Antibacterial cotton fabric grafted with silver nanoparticles and its excellent laundering durability. *Carbohydr Polym.* 2013;92(2):2088–94.
  159. Ghasemzadeh H, Mahboubi A, Karimi K. Full polysaccharide chitosan-CMC membrane and silver nanocomposite : synthesis , characterization , and antibacterial behaviors. *Polym Adv Technol.* 2016;27(9):1204–10.
  160. Pei M, Jia X, Zhao X, Li J, Liu P. Alginate-based cancer-associated, stimuli-driven and turn-on theranostic prodrug nanogel for cancer detection and treatment. *Carbohydr Polym.* 2018;183:131–9.
  161. Mocanu G, Nichifor M, Picton L, About-jaudet E, Cerf D Le. Preparation and characterization of anionic pullulan thermoassociative nanoparticles for drug delivery. *Carbohydr Polym.* 2014;111:892–900.
  162. Li L, Wang N, Jin X, Deng R, Nie S, Sun L, et al. Biodegradable and injectable in situ cross-linking chitosan-hyaluronic acid based hydrogels for postoperative adhesion prevention. *Biomaterials.* 2014;35(12):3903–17.
  163. Kiricsi I, Nagy JB, Verhoef MJ, Peters JA, Bekkum H Van. MCM-41 supported TEMPO as an environmentally friendly catalyst in alcohol oxidation. *Stud Surf Sci Catal.* 1999;125:465–72.
  164. Wu CN, Fuh SC, Lin SP, Lin YY, Chen HY, Liu JM, et al. TEMPO-Oxidized Bacterial Cellulose Pellicle with Silver Nanoparticles for Wound Dressing. *Biomacromolecules.* 2018;19(2):544–54.
  165. T. S. A, V. CS, F. S, Thomas JP. Effect of dual stimuli responsive dextran/nanocellulose polyelectrolyte complexes for chemophotothermal synergistic cancer therapy. *Int J Biol Macromol.* 2019;135:776–89.
  166. Fan H, Ji N, Zhao M, Xiong L, Sun Q. Interaction of bovine serum albumin with starch nanoparticles prepared by TEMPO-mediated oxidation. *Int J Biol Macromol.* 2015;78:333–8.
  167. Yan JK, Ma H Le, Cai PF, Zhang HN, Zhang Q, Hu NZ, et al. Structural characteristics and antioxidant activities of different families of 4-acetamido-

- TEMPO-oxidised curdlan. *Food Chem.* 2014;143:530–5.
168. Crandall JK, Shi Y, Burke CP, Buckley BR. Potassium Monoperoxysulfate. In: *Encyclopedia of Reagents for Organic Synthesis*. American Cancer Society; 2012.
  169. Ruan CQ, Gustafsson S, Strømme M, Mihranyan A, Lindh J. Cellulose nanofibers prepared via pretreatment based on Oxone<sup>®</sup> oxidation. *Molecules*. 2017;22(12):19–21.
  170. Baxter EW, Reitz AB. Reductive Aminations of Carbonyl Compounds with Borohydride and Borane Reducing Agents. In: *Organic Reactions*. American Cancer Society; 2004. p. 4–24.
  171. Dash R, Ragauskas AJ. Synthesis of a novel cellulose nanowhisker-based drug delivery system. *RSC Adv.* 2012;2:3403–9.
  172. Omtvedt LA, Dalheim M, Nielsen TT, Larsen KL, Strand BL, Aachmann FL. Efficient Grafting of Cyclodextrin to Alginate and Performance of the Hydrogel for Release of Model Drug. *Sci Rep.* 2019;9(1):9325.
  173. Banks SR, Enck K, Wright M, Opara EC, Welker ME. Chemical Modification of Alginate for Controlled Oral Drug Delivery. *J Agric Food Chem.* 2019;67(37):10481–8.
  174. Abedini F, Hosseinkhani H, Ismail M, Domb AJ, Omar AR, Chong PP, et al. Cationized dextran nanoparticle-encapsulated CXCR4-siRNA enhanced correlation between CXCR4 expression and serum alkaline phosphatase in a mouse model of colorectal cancer. *Int J Nanomedicine.* 2012;7:4159–68.
  175. Jelkmann M, Menzel C, Baus RA, Ausserhofer P, Baecker D, Gust R, et al. Chitosan: The One and Only? Aminated Cellulose as an Innovative Option for Primary Amino Groups Containing Polymers. *Biomacromolecules.* 2018;19(10):4059–67.
  176. Jelkmann M, Leichner C, Menzel C, Krebs V, Bernkop-Schnürch A. Cationic starch derivatives as mucoadhesive and soluble excipients in drug delivery. *Int J Pharm.* 2019;570:118664.
  177. Faizuloev E, Marova A, Nikonova A, Volkova I, Gorshkova M, Izumrudov V. Water-soluble N- [( 2-hydroxy-3-trimethylammonium ) propyl ] chitosan chloride as a nucleic acids vector for cell transfection. *Carbohydr Polym.* 2012;89(4):1088–94.
  178. Suflet DM, Popescu I, Pelin IM, Nicolescu A, Hitruc G. Cationic curdlan : Synthesis , characterization and application of quaternary ammonium salts of curdlan. *Carbohydr Polym.* 2015;123:396–405.
  179. Heinze T, Liebert T, Klüfers P, Meister F. Carboxymethylation of cellulose in unconventional media. *Cellulose.* 1999;6(2):153–65.
  180. Leong KH, Chung LY, Noordin MI, Mohamad K, Nishikawa M, Onuki Y, et al. Carboxymethylation of kappa-carrageenan for intestinal-targeted delivery of bioactive macromolecules. *Carbohydr Polym.* 2011;83(4):1507–15.
  181. Saboktakin MR, Tabatabaie RM, Maharramov A, Ramazanov MA. Synthesis and in vitro evaluation of carboxymethyl starch-chitosan nanoparticles as drug delivery

- system to the colon. *Int J Biol Macromol.* 2011;48(3):381–5.
182. Asmarandei I, Fundueanu G, Cristea M, Harabagiu V, Constantin M. Thermo- and pH-sensitive interpenetrating poly(N-isopropylacrylamide)/carboxymethyl pullulan network for drug delivery. *J Polym Res.* 2013;20:293.
  183. Kaity S, Ghosh A. Carboxymethylation of Locust Bean Gum: Application in Interpenetrating Polymer Network Microspheres for Controlled Drug Delivery. *Ind Eng Chem Res.* 2013;52(30):10033–45.
  184. Zeng K, Groth T, Zhang K. Recent Advances in Artificially Sulfated Polysaccharides for Applications in Cell Growth and Differentiation, Drug Delivery, and Tissue Engineering. *ChemBioChem.* 2019;20(6):737–46.
  185. Tian Q, Wang XH, Wang W, Zhang CN, Wang P, Yuan Z. Self-assembly and liver targeting of sulfated chitosan nanoparticles functionalized with glycyrrhetic acid. *Nanomedicine Nanotechnology, Biol Med.* 2012;8(6):870–9.
  186. Huang G, Huang H. The derivatization and antitumor mechanisms of polysaccharides. *Future Med Chem.* 2017;9(16):1931–8.
  187. Suflet DM, Nicolescu A, Popescu I, Chitanu GC. Phosphorylated polysaccharides. 3. Synthesis of phosphorylated curdlan and its polyelectrolyte behaviour compared with other phosphorylated polysaccharides. *Carbohydr Polym.* 2011;84(3):1176–81.
  188. Griesser J, Burtscher S, Köllner S, Nardin I, Prüfert F, Bernkop-Schnürch A. Zeta potential changing self-emulsifying drug delivery systems containing phosphorylated polysaccharides. *Eur J Pharm Biopharm.* 2017;119:264–70.
  189. Wei J, Xue W, Yu X, Qiu X, Liu Z. PH Sensitive phosphorylated chitosan hydrogel as vaccine delivery system for intramuscular immunization. *J Biomater Appl.* 2017;31(10):1358–69.
  190. Balakrishnan B, Lesieur S, Labarre D, Jayakrishnan A. Periodate oxidation of sodium alginate in water and in ethanol – water mixture : a comparative study. *Carbohydr Res.* 2005;340(7):1425–9.
  191. Sánchez AV, Gustavo J, Zárraga Á. Green Oxidation of Organic Compounds: manganese Sulphate/Oxone®/Water. *J Mex Chem Soc.* 2007;51(4):213–6.
  192. Rodriguez S, Vasquez L, Costa D, Romero A, Santos A. Oxidation of Orange G by persulfate activated by Fe(II), Fe(III) and zero valent iron (ZVI). *Chemosphere.* 2014;101:86–92.
  193. Bergman Y, Perlmutter P, Thienthong N. Solvent-free preparation of primary imines from ( 2-hydroxyaryl ) ketones. *Green Chem.* 2004;6(11):539–40.
  194. Sierakowski MR, Milas M, Desbrières J, Rinaudo M. Specific modifications of galactomannans. *Carbohydr Polym.* 2000;42(1):51–7.
  195. Azzam F, Galliot M, Putaux J-L, Heux L, Jean B. Surface peeling of cellulose nanocrystals resulting from periodate oxidation and reductive amination with water-soluble polymers. *Cellulose.* 2015;22(6):3701–14.
  196. Cheng LH, Nur Halawiah H, Lai BN, Yong HM, Ang SL. Ultrasound mediated acid hydrolysis of konjac glucomannan. *Int Food Res J.* 2010;17:1043–50.

197. Janssens J, Risseuw MDP, Van der Eycken J, Van Calenbergh S. Regioselective Ring Opening of 1,3-Dioxane-Type Acetals in Carbohydrates. *European J Org Chem.* 2018;2018(46):6405–31.
198. Peng Q, Zhang Z, Sun X, Zuo J, Zhao D, Gong T. Mechanisms of Phospholipid Complex Loaded Nanoparticles Enhancing the Oral Bioavailability. *Mol Pharm.* 2010;7(2):565–75.
199. Kristiansen KA, Pothast A, Christensen BE. Periodate oxidation of polysaccharides for modification of chemical and physical properties. *Carbohydr Res.* 2010;345(10):1264–71.